symmetry

MDPI

Article

Navigation Route Planning for Tourism Intelligent Connected Vehicle Based on the Symmetrical Spatial Clustering and Improved Fruit Fly Optimization Algorithm

Xiao Zhou [1,2], Jian Peng [1,*], Bowei Wen [3,*] and Mingzhan Su [3]

[1] College of Computer Science, Sichuan University, Chengdu 610065, China; zhouxiao@infu.ac.cn
[2] School of Culture and Tourism, Leshan Vocational and Technical College, Leshan 614000, China
[3] Institute of Geospatial Information, PLA Strategic Support Force Information Engineering University, Zhengzhou 450001, China; smzh625@infu.ac.cn
* Correspondence: jianpeng@scu.edu.cn (J.P.); gis0829@infu.ac.cn (B.W.)

Abstract: The intelligent connected vehicle (ICV) decision-making system needs to match tourist interests and search for the route with the lowest travel cost when recommending POIs (Points of Interest) and navigation tour routes. In response to this research objective, we construct a navigation route-planning model for tourism intelligent connected vehicles based on symmetrical spatial clustering and improved fruit fly optimization algorithm. Firstly, we construct the POI feature attribute clustering algorithm based on the spatial decision forest to achieve the optimal POI recommendation. Secondly, we construct the POI spatial attribute clustering algorithm based on the SA-AGNES (Spatial Accessibility-Agglomerative Nesting) to achieve the spatial modeling between POIs and ICV clusters. On the basis of POI feature attribute and spatial attribute, we construct the POI recommendation algorithm for the ICV navigation routes based on the attribute weights. On the basis of the recommended POIs, we construct the tourism ICV navigation route-planning model based on the improved fruit fly optimization algorithm. Experiments prove that the proposed algorithm can accurately output POIs that match tourists' interests and needs, and find out the ICV navigation route with the lowest travel cost. Compared with the commonly used map route-planning methods and traditional route-searching algorithms, the proposed algorithm can reduce the travel costs by 15.22% at most, which can also effectively reduce the energy consumption of the ICV system, and improve the efficiency of sight-seeing and traveling for tourists.

Keywords: symmetrical spatial clustering; improved fruit fly optimization algorithm; intelligent connected vehicle (ICV); tourism POI recommendation; tourism navigation route

Citation: Zhou, X.; Peng, J.; Wen, B.; Su, M. Navigation Route Planning for Tourism Intelligent Connected Vehicle Based on the Symmetrical Spatial Clustering and Improved Fruit Fly Optimization Algorithm. *Symmetry* **2024**, *16*, 159. https://doi.org/10.3390/sym16020159

Academic Editor: Peng-Yeng Yin

Received: 1 December 2023
Revised: 23 January 2024
Accepted: 27 January 2024
Published: 29 January 2024

1. Introduction

1.1. Research Background and Problem Discussion

The issue of tourism transportation is the key to smart tourism research. After arriving at the tourism destination city, tourists usually use different means of transportation such as public buses, subways, taxis, shared bicycles, etc., when transferring between different POIs in the city. When tourists use transportation modes to move and travel in the city, they will pay for the travel costs. As an important component of the tourism budget, travel cost will directly affect the total cost of tourists participating in tourism activities [1,2]. The lower the travel cost is, the lower the total cost for tourists will be, and the higher tourists' satisfaction will be. However, tourists are usually unfamiliar with the transportation conditions of the tourism cities; thus, it is difficult to achieve optimal routes by planning trips by themselves when choosing public transportation, making the cost control difficult. The appearance of intelligent connected vehicles (ICVs) has provided innovative ideas for smart tourism transportation planning and route recommendation. By designing the ICV decision-making system and route navigation system, it is possible to provide travel decisions for tourists,

guide them to follow the optimal routes to their destinations, and effectively control the travel costs, reduce tour expenses, and finally improve the tourists' satisfaction [3,4]. At present, the research on ICV routes mainly focuses on the following aspects: The first one is research on the perception and obstacle avoidance of ICVs to the surrounding environment. Through communication and interaction between ICVs and the surrounding objects, the obstacles appearing on the travel routes are avoided to ensure the smooth driving of ICVs. The second one is to integrate the ICV technology with the public transportation systems to achieve the intelligent operation of the public transportation. The third one is to study the route design and layout of the ICV-dedicated driving roads, especially how to ensure the smooth operation of the ICVs and the traditional public transportation under the coexistence of the two systems. For the construction of smart tourism, the integration of ICV navigation route research with smart tourism decision-making and route planning is currently weak and insufficient. There is no research on the introduction of ICV decision-making and navigation route-planning mechanisms into the smart tourism transportation, and there is also a lack of design and development of related algorithms. Meanwhile, there are several main problems in the research of smart tourism decision-making and tourism transportation routes. Firstly, there is insufficient research on the tourism decision-making of the destination POIs. When tourists are unfamiliar with the POIs of tourism cities, how to use the intelligent decision-making algorithms to achieve POI recommendations that best match the tourists' interests with the optimal spatial distributions is the key to meeting the tourists' motivation benefits. At present, there is insufficient research on the travel interests and spatial distributions of POIs in smart transportation routes, resulting in the POIs on the travel routes being unable to meet the tourists' interests. Secondly, the planning of intelligent tourism transportation routes has the features of subjectivity and blindness. The design of tourism transportation routes lacks studies on the geospatial constraints and traffic constraints, and there is also no research on the optimal routes under the condition of POI recommendations, resulting in higher costs for tourism transportation routes and higher travel costs for tourists.

In response to the current problems, we summarize the relationship between the optimal ICV routes and smart tourism with tourists, and the goal of this study is to construct the relationship between the optimal ICV routes and tourists.

(1) Relationship 1: The POIs on the ICV routes are the targets for tourists to visit. Whether the tourists can generate the maximum benefit motivation from visiting the POIs is an important evaluation indicator of whether the ICV routes are the optimal ones. Therefore, each POI on the optimal ICV route must be the one that the tourists are most interested in and willing to visit. By constructing the relationship between POI functional attributes and tourist interest attributes, we recommend POIs for tourists and establish the relationship between the ICV routes and the tourists' interests and demands.

(2) Relationship 2: From the perspective of energy conservation and travel cost control for the tourists, the ICVs will produce travel costs and fees in moving and ferrying tourists between different POIs, which will ultimately be paid by the tourists. From the perspective of saving travel costs, the ICV routes are directly related to tourist motivation benefits. The key to improving tourist satisfaction is to search for the ICV routes with the best POIs and the lowest travel cost. Thus, the modeling for the optimal ICV routes has close relationship to the tourists' satisfaction.

1.2. Problem Solving Methods

In response to the research background and the existing problems of intelligent tourism transportation and ICVs, we propose the following solutions. Firstly, in response to the insufficient research on the destination POI decision-making, an intelligent decision-making system for POI recommendation should be constructed. The ICVs in smart tourism transportation play a role in guiding tourists to reach their destinations; thus, the design of navigation routes should be based on POI recommendations. That is, the premise of the

tourism ICV navigation route is to determine the POIs on the route that meet the interests and needs of tourists. Therefore, recommending POIs that meet tourists' interests and have the optimal spatial distributions for tourists is the core function of constructing a tourism ICV intelligent decision-making system. There are two steps to solving this problem. One is to construct a POI clustering algorithm based on feature attributes, mining the matching relationship between the POI feature attributes and the tourists' interests, and recommending the POIs with the highest attribute matching degrees; the second is to construct the POI spatial clustering algorithm centered around the tourism ICV transfer stations, and obtain the POIs with the best spatial distributions from the POIs with the highest attribute matching degrees through the spatial accessibility search, ultimately utilizing the POIs to construct the tourism ICV navigation route algorithm. Secondly, in response to the problems of subjectivity and blindness in planning the intelligent ICV navigation routes, it is necessary to consider the geospatial constraints and basic transportation facilities of the destination cities, such as POI distributions, road distributions, and spatial distances, etc. Based on the modeling background of these constraints, the ICV navigation routes should be constructed based on the recommended POIs, so as to minimize the travel cost of the tourism ICV navigation route and reduce the travel time spent by tourists on the road and ICV energy consumption, then finally improve the tourists' satisfaction.

2. Related Work and Analysis

2.1. Related Work and Limitation

Representative studies on the ICV route problems and intelligent tourism transportation route-planning mainly include the following: Hou et al. [5] proposed a route-planning mechanism based on deep reinforcement learning (DRL). A deep reinforcement learning model was established using Rainbow DQN, and the prioritized successive decision-making route-planning method was designed. It prioritized emergency vehicles, public transportation vehicles and other general vehicles in the city, and verified the effectiveness of the constructed route-planning method in different experimental scenarios. Noussaiba et al. [6] constructed a heterogeneous algorithm called Ant Colony Optimization with Pheromone Termites (ACO-PT), which combined two state-of-the-art algorithms, namely Pheromone Termites (PT) and Ant Colony Optimization (ACO), to address efficient routing to improve energy efficiency, increase throughput, and shorten end-to-end latency. Wang et al. [7] proposed an adaptive adjustment mechanism to address the typical problems of weak global optimization ability, easy falling into local optimization and slow convergence speed in the intelligent vehicle route solving algorithms, and improved the Whale optimization algorithm to enhance its operational ability. It has better convergence ability compared to other algorithms. Liu et al. [8] innovatively introduced a bidding mechanism in the scenario of connected vehicles and proposed a new dynamic route-planning method. Experiments showed that in large-scale traffic flow scenarios, the bidding mechanism was beneficial for improving the transportation efficiency of the road network. Kurdi et al. [9] introduced a path planning algorithm inspired by the natural tidal phenomena—Tidal Path Planning (TPP). The concept of gravity between the Earth and the Moon was adopted to avoid searching blocked routes and to find a shortest path. Compared to other optimal path algorithms, this algorithm had higher execution efficiency. Xu et al. [10] proposed a personalized path planning model based on the urgency situation. The experimental results showed that this algorithm could not only plan routes with different functions for different users, but also plan personalized routes by different user preferences. Shan [11] proposed an ant colony optimization algorithm to solve the problem of the optimal tourism route planning. Based on the basic ant colony optimization algorithm, an optimized pheromone update strategy was proposed. Experiments made comparisons of the effects of different optimization algorithms in tourism route planning, and the acceleration ratio of the optimized ant colony algorithm was tested using the graphics processing unit parallel computing program. The results showed that the proposed algorithm provided certain advantages and had potential applications in parallel computing. Damos et al. [12] proposed a novel urban

tourism path planning method based on a multi-objective genetic algorithm, with the main goal of enhancing the accuracy of the genetic algorithm (GA) by adopting new parameters and selecting the optimal tourism path by combining external and internal tourist site potentials. Compared with existing tourism path planning methods, this method is more accurate and straightforward than other methods when choosing routes.

Through the analysis of related work, it can be concluded that current studies on ICV route-planning mainly focus on the following aspects. The first one is optimizing the existing route algorithms to improve their execution efficiency. By introducing new variables, changing the structure of the algorithm, or adding new mechanisms, the execution process of the original algorithm is changed, thereby the execution speed of the algorithm is optimized. The second one is to classify the different vehicles within the city, measure their priorities in the urban transportation system, and plan different routes based on the priority level of the vehicles. The third one is to design new algorithms and use them to search for the optimal path, providing new research methods for the tourism transportation route planning. These tourism transportation route planning methods have a certain degree of innovation, and have solved several problems in the current operation of tourism vehicles and optimal tour route planning. However, from the perspective of satisfying the interests and needs of individual tourists and controlling the cost of tour routes, these studies still have some shortcomings, which are mainly reflected in the following two aspects:

Firstly, the research on matching of tourists' interests with POI attributes is insufficient. The core problem of tourism ICV route planning still relies on the selection and matching of route nodes; that is, how to search for the POIs that best match tourists' interests from numerous tourist destinations and use them as the control points for tourism ICV navigation routes. Due to the fact that POIs have both feature attributes and spatial attributes, it is a precondition for ICV tourism route planning to recommend the POIs with the best feature attributes and spatial attributes for tourists. Secondly, the research on ICV route costs is insufficient. The planning of the tourism ICV navigation routes is influenced by geospatial constraints, such as POI geographical location, ICV starting point, ICV terminal point, ICV transfer station location, road spatial distribution, and road distance, etc. The planning of tourism ICV navigation routes must consider the real-world spatial environment, and it is necessary to design the optimization algorithm under these geospatial constraints to output the routes with the lowest ICV travel cost.

2.2. The Difference and Advantage of Our Proposed Work

The gaps between our proposed model and related work, as well as the advantages of the proposed work, are mainly reflected in the following aspects: Reference [5] focuses on constructing the deep learning algorithm to achieve priority sorting of vehicles of different levels, without considering the fairness of tourist services. Our method reflects the fairness of all ICVs and ICV routes, allowing each tourist to enjoy the same POI recommendations and ICV route planning services. Reference [6] focuses on studying the shortest route-searching model based on the improved ant colony algorithm, and has conducted extensive research on algorithm optimization. Our method aims to search for the POIs that best match the interests of tourists, and on this basis, search for the optimal ICV routes connecting the POIs. It is not aimed at improving a certain algorithm, but at building a new method with the goal of tourist interests and reducing travel costs. Reference [7] also optimizes and improves the algorithm to improve its convergence performance, which is different from the goal of the method we constructed. Reference [8] is mainly aimed at optimizing the transportation efficiency of the road network and improving the transportation capacity of vehicles. Our method has different research objectives, aiming to match tourist interests and reduce travel costs. Reference [9] optimizes and improves the algorithm to improve its execution efficiency, which is different from the goal of the method we proposed. Execution efficiency is not our research goal. Within a tolerable range of algorithm runtime, our constructed method places more emphasis on the matching degree between POIs and tourist interests, as well as the overall cost of ICV routes. Reference [10] constructs a model

based on the urgency of tourism, which has strong constraints on travel time. It is also different from the method we constructed. Our method assumes that tourists have sufficient travel time and budget, and from the perspective of fair recommendation, it matches the optimal POIs for tourists and searches for optimal routes. Both references [11,12] aim to optimize intelligent algorithms with the aim of improving their accuracy. This research method does not start from the personalized needs of tourists and it ignores the matching of POI feature attributes with tourist interests. Our method focuses on matching tourist interests, reducing ICV route costs and improving tourist satisfaction.

2.3. Our Proposed Method

Based on the analysis of the problems, we propose and construct a navigation route-planning model for the tourism intelligent connected vehicle based on symmetrical spatial clustering and the improved fruit fly optimization algorithm. The main studies and contributions are as follows. Figure 1 shows the main research ideas and content architecture of our work.

(1) We construct a POI feature attribute clustering algorithm based on the spatial decision forest, which clusters the urban POIs according to the root nodes with different natural attributes. The binary tree algorithm with the descending matching degree of tourists' interests is proposed to generate a spatial decision tree. Each decision tree represents one feature attribute cluster. The construction of the spatial decision forest can output the POIs that best match tourists' interests for ICVs.

(2) We also construct a POI spatial attribute clustering algorithm based on the spatial accessibility and AGNES (SA-AGNES). Taking the ICV transfer stations as the core points of AGNES spatial clustering, the spatial attributes of POIs within the neighborhood of the transfer stations are determined by searching spatial accessibility, and the POIs are spatially clustered to determine the spatial relationship between the ICV transfer stations and neighboring POIs. Finally, the ICV intelligent decision-making system will output the POIs with the optimal spatial distributions.

(3) We design and construct an optimal POI recommendation algorithm based on spatial clustering. In response to the control node selection problem of the tourism ICV navigation route-planning algorithm, we set the searching target as the POIs that best match tourists' interests and have the optimal spatial distributions. The ICV intelligent decision-making system searches for POIs that tourists need to visit, and uses them as the precondition for the ICV route-planning algorithm.

(4) Based on the modeling of the urban geospatial environment and traffic road conditions, we construct a tourism ICV navigation route model based on the improved fruit fly optimization algorithm. Using the ICV transfer stations and POIs as nodes, it outputs the tour route with the lowest travel cost under the geospatial constraints.

(5) We design and perform the validation experiment and comparative experiment, which proves that the proposed algorithm can accurately output POIs that match tourists' interests, and can find out the ICV navigation route with the lowest travel cost. Compared with the commonly used map route-planning methods and the traditional route-searching algorithms, the proposed algorithm can reduce the travel cost by 15.22% at most, and effectively reduce energy consumption of the ICV system, then finally improve the tourists' satisfaction.

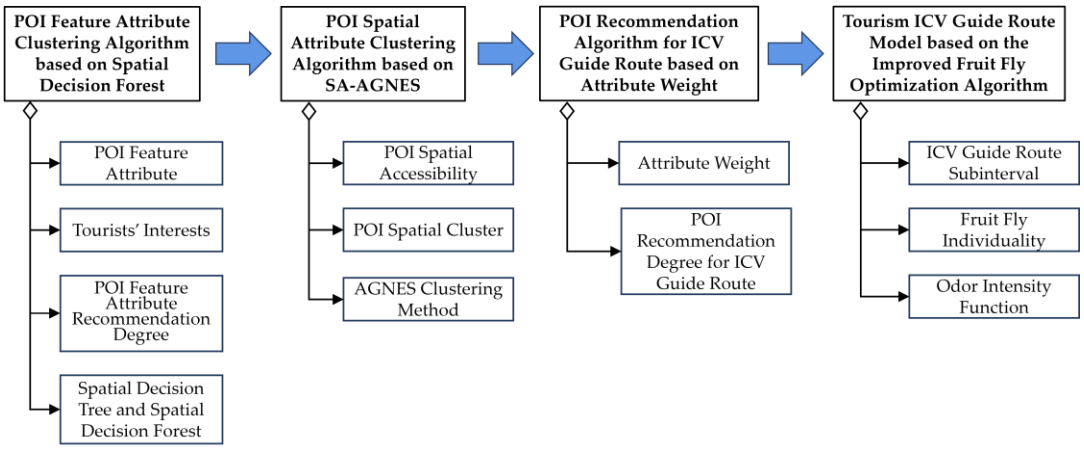

Figure 1. The main research ideas and content architecture of our work.

3. Methodology

3.1. The Optimal POI Recommendation Algorithm for Tourism ICV System

This section consists of three parts. We firstly construct a POI feature attribute clustering algorithm in Section 3.1.1, with the aim of establishing a matching relationship between the tourist interest needs and POI feature attributes. Secondly, in Section 3.1.2, we construct a POI spatial attribute clustering algorithm with the aim of establishing the spatial relationship between POIs and ICV transfer stations. Based on the two types of models in Sections 3.1.2 and 3.1.3, we introduce the concept of attribute weight and construct a POI recommendation algorithm based on attribute weights in Section 3.1.3. The aim is to recommend POIs with feature attributes that best match the interests of tourists and achieve optimal spatial distribution and spatial accessibility. According to the modeling conditions as per the POI feature attribute clustering algorithm, the POI natural classification, POI feature attribute and POI feature attribute recommendation degree are the three most important attributes. As per the POI spatial attribute clustering algorithm, the POI spatial accessibility and POI spatial cluster are the two most important attributes. As per the POI recommendation algorithm based on the attribute weight, the attribute weight factor and POI recommendation degree are the two most important attributes.

3.1.1. POI Feature Attribute Clustering Algorithm Based on Spatial Decision Forest

According to the characteristics, POIs could be divided into natural classifications such as "park and green land", "culture and history", "leisure shopping" and "amusement and theme park". A single POI has feature attributes that affect tourists' interests and play a decisive role in selecting POIs, such as "travel cost", "travel time", "POI level", and "POI popularity", etc., which constitute the key factors for recommending POIs in the tourism ICV intelligent decision-making system. The key to recommending POIs for tourists traveling in cities using ICVs is to obtain their interest needs and construct a matching relationship between the tourists' interests and the POI feature attributes [13–15]. Based on the ICV decision objectives, we construct a POI feature attribute clustering algorithm based on the spatial decision forest. In the algorithm, the POI natural classification, POI feature attribute and POI feature attribute recommendation degree are the three most important attributes.

In tourism activities, the characteristics of POIs that attract tourists to make choices and reflect the basic tourism functions are the POI natural attribute classifications, denoted as $G_{N(i)}$, $0 < i \leq k_1$, $i, k_1 \in \mathbf{N}$, in which k_1 is the total number of the natural attribute classification.

The factors that affect tourists' interests and determine whether to choose POIs for sightseeing are the POI feature attribute factors, denoted as $f_{P(i)}$, $0 < i \leq k_2$, $i, k_2 \in \mathbf{N}$, in which k_2 is the total number of the feature attribute. The POI feature attribute factor is

the key to determining tourists' interest choices and recommending POIs. To construct a POI interest matching algorithm, it is necessary to quantify and store the POI feature attribute factors in a structured format. Construct a $k_2 \times 1$ dimension column vector to store k_2 number of feature attribute factors $f_{P(i)}$ and perform initial quantization. Set this structured vector as the POI feature attribute vector, denoted as $\mathbf{f}_{P(i)}$. Each element $f_{P(i)}$ in vector $\mathbf{f}_{P(i)}$ has different quantization interval $f_{P(i,j)}$, each $f_{P(i,j)}$ represents the feature measurement of the factor $f_{P(i)}$, and each quantization interval $f_{P(i,j)}$ is a subset of the factor $f_{P(i)}$ and is independent from each other. Using the row elements $f_{P(i)}$ of the column vector $\mathbf{f}_{P(i)}$ as the initial growth element, the feature measurements $f_{P(i,j)}$ are extended to the column elements of each row to form a $k_2 \times l$ dimension matrix, $0 < l \leq \max l$, $l \in \mathbf{N}$. The quantization interval matrix is defined as the POI feature attribute matrix, denoted as $\mathbf{f}_{P(i,j)}$.

We construct the POI feature attribute vector $\mathbf{f}_{P(i)}$ and the POI feature attribute matrix $\mathbf{f}_{P(i,j)}$ using Formulas (1) and (2).

$$\mathbf{f}_{P(i)} = \left\langle f_{P(1)}, \quad f_{P(2)}, \quad \ldots, \quad f_{P(k_2)}, \right\rangle^T \tag{1}$$

$$\mathbf{f}_{P(i,j)} = \begin{bmatrix} f_{P(1,1)} & f_{P(1,2)} & \cdots & f_{P(1,l)} \\ f_{P(2,1)} & f_{P(2,2)} & \cdots & f_{P(2,l)} \\ \cdots & \cdots & \cdots & \cdots \\ f_{P(k_2,1)} & f_{P(k_2,2)} & \cdots & f_{P(k_2,l)} \end{bmatrix} \tag{2}$$

Using the equivalent factor $f_{T(i)}$ corresponding to the POI feature attribute factor $f_{P(i)}$ as the element, we construct a $k_2 \times 1$ dimension column vector representing the quantitative tourists' interests in POI feature attributes. Set this column vector as the tourist interest measurement vector, denoted as $\mathbf{f}_{T(i)}$. The element in the vector $\mathbf{f}_{T(i)}$ is the tourist interest factor $f_{T(i)}$, which corresponds to the POI feature attribute factor $f_{P(i)}$. Using the row elements $f_{T(i)}$ of the column vector $\mathbf{f}_{T(i)}$ as the initial growth elements, the feature measurement $f_{T(i,j)}$ is extended to the column element of each row to form a $k_2 \times l$ dimension matrix, $0 < l \leq \max l$, $l \in \mathbf{N}$, and the quantization interval matrix is the tourist interest measurement matrix, denoted as $\mathbf{f}_{T(i,j)}$. Matrix $\mathbf{f}_{T(i,j)}$ is the correlating matrix for the matrix $\mathbf{f}_{P(i,j)}$, and its data structure is the same as $\mathbf{f}_{P(i,j)}$. Formulas (3) and (4) represent the tourist interest measurement vector $\mathbf{f}_{T(i)}$ and tourist interest measurement matrix $\mathbf{f}_{T(i,j)}$.

Before taking the ICV to the POI, the tourists need to input interest factors and corresponding quantitative values into the ICV intelligent decision-making system. The ICV intelligent decision-making system quantifies the vector $\mathbf{f}_{T(i)}$ as the basic interest needs of tourists. The tourists firstly select factors $f_{T(i)}$ from the matrix $\mathbf{f}_{T(i,j)}$, and then determine the specific quantization value for each factor $f_{T(i)}$ to generate a quantization vector $\mathbf{f}_{T(i)}$.

$$\mathbf{f}_{T(i)} = \left\langle f_{T(1)}, \quad f_{T(2)}, \quad \ldots, \quad f_{T(k_2)}, \right\rangle^T \tag{3}$$

$$\mathbf{f}_{T(i,j)} = \begin{bmatrix} f_{T(1,1)} & f_{T(1,2)} & \cdots & f_{T(1,l)} \\ f_{T(2,1)} & f_{T(2,2)} & \cdots & f_{T(2,l)} \\ \cdots & \cdots & \cdots & \cdots \\ f_{T(k_2,1)} & f_{T(k_2,2)} & \cdots & f_{T(k_2,l)} \end{bmatrix} \tag{4}$$

When the classifications i for $f_{P(i,j)}$ and $f_{T(i,j)}$ of matrix $\mathbf{f}_{P(i,j)}$ and $\mathbf{f}_{T(i,j)}$ are different, the quantization intervals have different orders of magnitude. To ensure that each classification has the same order of magnitude effect on POI interest matching, we introduce a POI recommendation disturbance factor $\delta_{(i)}$ to normalize the factors $f_{P(i,j)}$ and $f_{T(i,j)}$. The ICV intelligent decision-making system determines the recommendation degree of POI by judging the spatial closeness between the tourist interest measurement vector $\mathbf{f}_{T(i)}$ and the POI feature attribute vector $\mathbf{f}_{P(i)}$, and then recommends the POIs with the best matched feature attributes for tourists. Formulas (5) and (6) represent the POI recommendation

function $\zeta(\mathbf{f}_{T(i)}, \mathbf{f}_{P(i)})$ constructed by introducing the recommendation disturbance factor $\delta_{(i)}$, in which i is traversed $i \sim (0, k_2)$, $i, k_2 \in \mathbf{N}$.

$$\zeta(\mathbf{f}_{T(i)}, \mathbf{f}_{P(i)}) = \frac{1}{\left\| \delta_{(i)} \cdot \left(\mathbf{f}_{P(i)} - \mathbf{f}_{T(i)} \right) \right\|_p + 1} \tag{5}$$

$$\zeta(\mathbf{f}_{T(i)}, \mathbf{f}_{P(i)}) = \frac{1}{\left(\sum_{i=1}^{k_2} \left| \delta_{(i)} \cdot f_{P(i)} - \delta_{(i)} \cdot f_{T(i)} \right|^p \right)^{\frac{1}{p}} + 1} \tag{6}$$

Construct a complete binary tree with the natural classification $G_{N(i)}$ as the root node and the POI feature attribute recommendation degrees $\zeta(\mathbf{f}_{T(i)}, \mathbf{f}_{P(i)})$ in descending order as the child nodes. This binary tree is the spatial decision tree based on the feature attribute recommendation, denoted as $\mathbf{t}_{ree \cdot G_{N(i)}}$. The decision forest composed of spatial decision trees $\mathbf{t}_{ree \cdot G_{N(i)}}$ generated by k_1 number of natural classifications $G_{N(i)}$ is defined as a spatial decision forest based on the feature attribute recommendation, denoted as $\mathbf{f}_{orest \cdot G_{N(i)}}$.

The POI feature attribute clustering algorithm based on the spatial decision forest is constructed as follows (Algorithm 1). Figure 2 shows the schematic diagram of the process for constructing the feature attribute clustering algorithm:

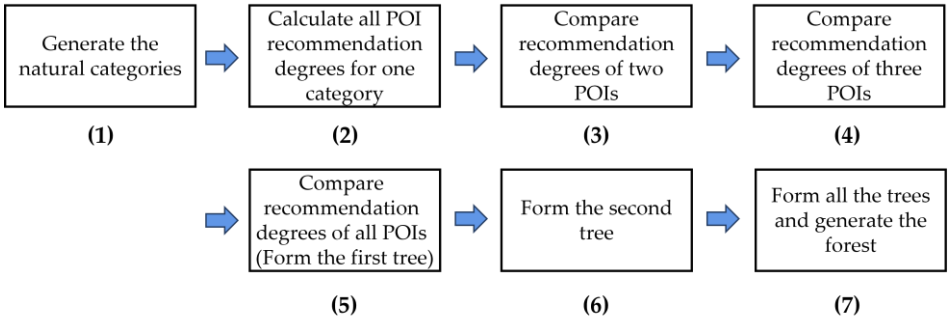

Figure 2. The process for constructing the feature attribute clustering algorithm.

Subfigure (1) shows the first step of the algorithm: generating the natural attribute labels;

Subfigure (2) shows the second step of the algorithm: taking the first natural attribute as an example, calculate the recommendation degrees $\zeta_{(x)}$ of all POIs for the attribute;

Subfigure (3) shows the third step of the algorithm: comparing the recommendation degrees $\zeta_{(1)}$ and $\zeta_{(2)}$ of the first POI and the second POI, with the larger value stored in the root node and the smaller value stored in the left child node of the lower level;

Subfigure (4) shows the fourth step of the algorithm: adding the third POI recommendation degree $\zeta_{(3)}$, comparing $\zeta_{(1)}$, $\zeta_{(2)}$ and $\zeta_{(3)}$. The maximum value is stored at the root node, the second maximum value is stored at the leftmost child node of the lower level, and the minimum value is stored at the rightmost child node of the lower level;

Subfigure (5) shows the fifth step of the algorithm: comparing the recommendation degrees of all POIs. The larger value is stored in the upper level or left child node, and the smaller value is stored in the lower level or right child node, so that the recommendation degree of any upper-level child node is greater than that of the lower level, and the recommendation degree of any left child node in any level is larger than that of the right child node;

Subfigure (6) shows the sixth step of the algorithm: constructing the second decision tree;

Subfigure (7) shows the seventh step of the algorithm: constructing the decision trees for all the natural attributes to form a decision forest.

Figure 3 shows a spatial decision forest $\mathbf{f}_{orest \cdot G_{N(i)}}$ constructed by k_1 number of spatial decision trees.

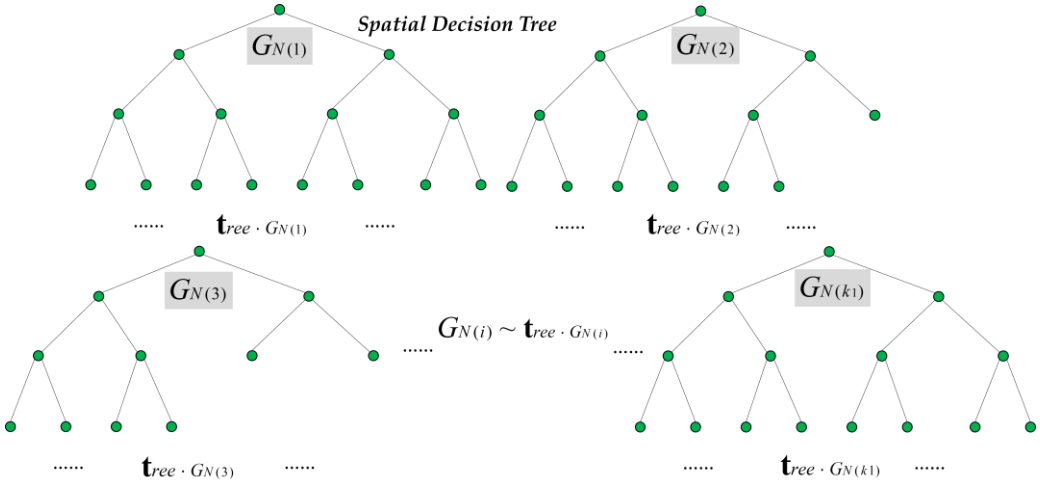

Figure 3. The k_1 number of decision tress $\mathbf{t}_{ree \cdot G_{N(i)}}$ consists of the spatial decision forest $\mathbf{f}_{orest \cdot G_{N(i)}}$.

Algorithm 1: The POI feature attribute clustering algorithm based on spatial decision forest $\mathbf{f}_{orest \cdot G_{N(i)}}$

Input: POI natural attribute $G_{N(i)}$ root nodes, POI feature attribute vector $\mathbf{f}_{P(i)}$, POI feature attribute matrix $\mathbf{f}_{P(i,j)}$, tourist interest measurement vector $\mathbf{f}_{T(i)}$, tourist interest measurement matrix $\mathbf{f}_{T(i,j)}$, disturbance factor $\delta_{(i)}$

Output: Spatial decision forest $\mathbf{f}_{orest \cdot G_{N(i)}}$

Step 1: As to attribute $G_{N(i)}$, take $i = 1$, construct spatial decision tree $\mathbf{t}_{ree \cdot G_{N(1)}}$. Obtain POIs that meet $P_{(x)} \in G_{N(1)}$, encode the POIs $P_{(x)}$, $x \in (0, h_1]$, $x, h_1 \in \mathbf{N}$.

Step 2: Calculate the $\zeta(\mathbf{f}_{T(i)}, \mathbf{f}_{P(1)}) \sim \zeta_{(x)}$, x traverses $x \in (0, h_1]$, then output h_1 number of recommendation degrees $\zeta(\mathbf{f}_{T(i)}, \mathbf{f}_{P(1)}) \sim \zeta_{(x)}$.

Step 3: Compare $\zeta_{(1)}$ and $\zeta_{(2)}$, iterating $x = x + 1$:

(1) Search max$\zeta_{(x)}$, store into $N_{ode(1,1)}$;

(2) Search min$\zeta_{(x)}$, store into $N_{ode(2,1)}$.

Step 4: Add $\zeta_{(3)}$, compare $\zeta_{(1)}$, $\zeta_{(2)}$, and $\zeta_{(3)}$, iterating $x = x + 1$:

(1) Search max$\zeta_{(x)}$, store into $N_{ode(1,1)}$;

(2) Search submax$\zeta_{(x)}$ and store into $N_{ode(2,1)}$;

(3) Search min$\zeta_{(x)}$, store into $N_{ode(2,2)}$.

Step 5: Return to Step 3, in line with the same algorithm from Step 3 to Step 4, add $\zeta_{(x)}$, compare $\zeta_{(1)}, \zeta_{(2)}, \ldots, \zeta_{(x)}$, store recommendation degree $\zeta_{(x)}$ into node $N_{ode(\alpha,\beta)}$, in descending order sort algorithm of decision tree $\mathbf{t}_{ree \cdot G_{N(1)}}$, iterating $x = x + 1$. When iterating of x meets $x = h_1$, the algorithm ends. Output $\mathbf{t}_{ree \cdot G_{N(1)}}$.

Step 6: Turn back to Step 1. As to attribute $G_{N(i)}$, take $i = 2$. In line with the same algorithm from Step 2 to Step 5, construct the spatial decision tree $\mathbf{t}_{ree \cdot G_{N(2)}}$.

Step 7: As to attribute $G_{N(i)}$, traverse $i \in (2, k_1]$, output $\mathbf{t}_{ree \cdot G_{N(3)}}$, $\mathbf{t}_{ree \cdot G_{N(4)}}, \ldots, \mathbf{t}_{ree \cdot G_{N(k_1)}}$, relating to k_1 number of natural clusters $G_{N(i)}$. The k_1 number of decision tress $\mathbf{t}_{ree \cdot G_{N(i)}}$ consists of the spatial decision forest $\mathbf{f}_{orest \cdot G_{N(i)}}$. The algorithm ends.

3.1.2. POI Spatial Attribute Clustering Algorithm Based on SA-AGNES

When the ICVs move in the city and search for POIs, in addition to matching the feature attributes of POIs, they should also consider the geospatial attributes of POIs, namely the spatial relationship between POIs and ICVs, in order to recommend the POIs with best spatial accessibility for tourists. In the design of the urban ICV systems, the ICV transfer stations can serve as the starting and ending points of the ICV navigation routes. That is,

the tourists take ICVs from the transfer stations to various POIs for sightseeing, and finally return to the nearest ICV transfer stations to the destination POIs. The entire process forms a complete ICV navigation route [16–18]. Therefore, a spatial relationship model between the POI and the ICV transfer stations is constructed, and then a POI spatial attribute clustering algorithm is constructed based on the spatial relationship to recommend the optimal POIs for the tourists. According to the modeling idea, in this section, we construct the POI spatial attribute clustering algorithm based on the SA-AGNES. In the algorithm, the POI spatial accessibility and POI spatial cluster are the two most important attributes.

The spatial accessibility (SA) between a certain ICV transfer station $IS_{(i)}$ and the POI $P_{(i)}$ in the urban ICV system is determined by the coordinates of $IS_{(i)}$ and $P_{(i)}$, representing the degree of spatial obstruction from the ICV transfer station $IS_{(i)}$ to the POI $P_{(i)}$, denoted as $S_{A(IS_{(i)},P_{(i)})}$. The higher the spatial accessibility is, the lower the travel cost from the ICV to the POI $P_{(i)}$ will be, and vice versa. Formula (7) is the constructed POI spatial accessibility model $S_{A(IS_{(i)},P_{(i)})}$, in which $(x \cdot IS_{(i)}, y \cdot IS_{(i)})$ is the coordinate of the ICV transfer station $IS_{(i)}$ in the urban geographic space and $(x \cdot P_{(i)}, y \cdot P_{(i)})$ is the coordinate of the POI in the urban geographic space. Figure 4 shows the constructed POI spatial accessibility model $S_{A(IS_{(i)},P_{(i)})}$.

$$S_{A(IS_{(i)},P_{(i)})} = \left|(x \cdot IS_{(i)} - x \cdot P_{(i)})^2 + (y \cdot IS_{(i)} - y \cdot P_{(i)})^2\right|^{-\frac{1}{2}} \tag{7}$$

The g number of POIs in the city are clustered based on their spatial accessibility $S_{A(IS_{(i)},P_{(i)})}$ to the ICV transfer stations $IS_{(i)}$, and the k number of generated clusters are POI spatial clusters, denoted as $C_{(i)}$. To construct a spatial clustering algorithm, the k number of ICV transfer stations $IS_{(i)}$ in the city are set as the seed points of POI spatial clusters $C_{(i)}$, denoted as $s_{eed(i)}$. Each cluster contains and only contains one seed point $s_{eed(i)}$, and the cluster contains $g_{(i)}$ number of POIs, and there is $i \in (0, k]$, $i, k \in \mathbf{N}$.

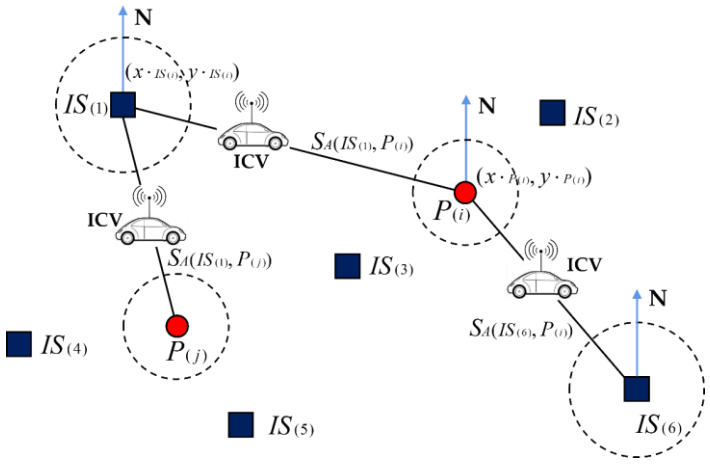

Figure 4. The constructed POI spatial accessibility model $S_{A(IS_{(i)},P_{(i)})}$.

Take the cluster $C_{(i)}$ as the matrix row, the cluster element $C_{(i,j)} \sim P_{(i)}$ as the matrix column, the seed point $s_{eed(i)}$ of each cluster $C_{(i)}$ as the first element of each row, then we generate a $k \times \left(1 + \max g_{(i)}\right)$ dimension matrix, and it is the POI spatial clustering matrix, denoted as $\mathbf{C}_{(i,j)}$, $i \in (0, k]$, $j \in (0, \max g_{(i)}]$, $i, j, k, g_{(i)} \in \mathbf{N}$. Formula (8) is the constructed POI spatial clustering matrix $\mathbf{C}_{(i,j)}$, with $C_{(i,1)}$ corresponding to $s_{eed(i)} \sim IS_{(i)}$. Formulas (9) and (10) represent the spatial accessibility $S_{A(IS_{(i)},P_{(i)})} \sim S_{A(i,j)}$ topological matrix $\mathbf{S}_{A(i,j)}{}^{*}$

of the POI $P_{(i)}$ corresponding to the matrix $\mathbf{C}_{(i,j)}$, $\mathbf{C}_{(i,1)}{}^{T}$, the cluster seed point $s_{eed(i)}$ is the column vector, and $\mathbf{S}_{A(i,j)}$ is the accessibility matrix.

$$\mathbf{C}_{(i,j)} = \begin{bmatrix} C_{(1,1)} & C_{(1,2)} & \cdots & C_{(1,g_{(1)})} \\ C_{(2,1)} & C_{(2,2)} & \cdots & C_{(2,g_{(2)})} \\ \cdots & \cdots & \cdots & \cdots \\ C_{(k,1)} & C_{(k,2)} & \cdots & C_{(k,g_{(k)})} \end{bmatrix} \tag{8}$$

$$\mathbf{S}_{A(i,j)}{}^{*} = \left[\mathbf{C}_{(i,1)}{}^{T}, \ \mathbf{S}_{A(i,j)}\right] \tag{9}$$

$$\mathbf{S}_{A(i,j)}{}^{*} = \begin{bmatrix} C_{(1,1)} & S_{A(1,2)} & \cdots & S_{A(1,g_{(1)})} \\ C_{(2,1)} & S_{A(2,2)} & \cdots & S_{A(2,g_{(2)})} \\ \cdots & \cdots & \cdots & \cdots \\ C_{(k,1)} & S_{A(k,2)} & \cdots & S_{A(k,g_{(k)})} \end{bmatrix} \tag{10}$$

The POI spatial attribute clustering algorithm based on the SA-AGNES is constructed as follows (Algorithm 2). Figure 5 shows the process for constructing the cluster matrix algorithm:

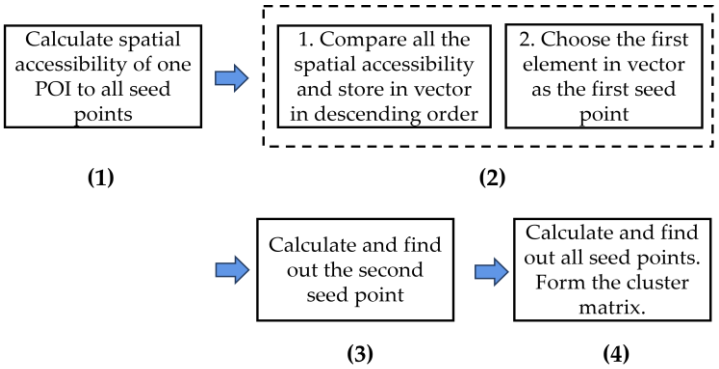

Figure 5. The process for constructing the cluster matrix algorithm.

Subfigure (1) shows the first step of the algorithm: calculating the spatial accessibility $S_{A(IS_{(i)})}$ between the first POI and the k number of ICV seed points $s_{eed(i)}$;

Subfigure (2) shows the second step of the algorithm: comparing the k number of spatial accessibility and storing them in the transition vector ${}^{\Delta}\mathbf{S}_{A}$. The larger value is stored in the front element of the vector, and the smaller value is stored at the back element of the vector; take the ICV corresponding to the first element as the seed point to the POI. The POI belongs to the cluster where the ICV is located and is stored in the corresponding row element of $\mathbf{S}_{A(i,j)}{}^{*}$;

Subfigure (3) shows the third step of the algorithm: calculating the ICV seed point corresponding to the maximum spatial accessibility value of the second POI. The POI belongs to the cluster where the ICV is located and is stored in the corresponding row element of $\mathbf{S}_{A(i,j)}{}^{*}$;

Subfigure (4) shows the algorithm's steps 4 to 5: generating the full ranked $\mathbf{S}_{A(i,j)}{}^{*}$.

Combined with the output topological matrix $\mathbf{S}_{A(i,j)}{}^{*}$, the topological forest $\mathbf{f}_{orest \cdot G_{N(i)}}{}^{*}$ with the labeled spatial accessibility $S_{A(IS_{(i)},P_{(i)})}$ is generated on the basis of the decision forest $\mathbf{f}_{orest \cdot G_{N(i)}}$, as shown in the Figure 6. An example of the POI spatial cluster constructed by matrix $\mathbf{S}_{A(i,j)}{}^{*}$ is shown in the Figure 7.

Algorithm 2: The POI spatial attribute clustering algorithm based on SA-AGNES

Input: k number of coordinates $(x \cdot IS_{(i)}, y \cdot IS_{(i)})$ of ICV transfer stations $IS_{(i)}$, g number of coordinates $(x \cdot P_{(i)}, y \cdot P_{(i)})$ of POIs $P_{(i)}$, the initialized seed points $s_{eed(i)}$, and the initialized zero matrix $\mathbf{O}_{\mathbf{S}A(i,j)*}$ for the $k \times \left(1 + \max g_{(i)}\right)$ dimension matrix ${\mathbf{S}_{A(i,j)}}^*$. Initialize the $1 \times k$ dimension transition vector ${}^{\Delta}\mathbf{S}_A$ for spatial accessibility.

Output: Full ranked matrix ${\mathbf{S}_{A(i,j)}}^*$ for cluster.

Step 1: As to g number of POIs $P_{(i)}$, take $i = 1$, calculate the $S_{A(IS_{(i)},P_{(1)})} \sim S_{A(IS_{(i)})}$ between $P_{(1)}$ and k number of seed points $s_{eed(i)}$.

Step 2: Compare k number of $S_{A(IS_{(i)})}$, in which i traverses $i \in (0, k]$, $i, k \in \mathbf{N}$.

Step 2.1: Compare $S_{A(IS_{(1)})}$ and $S_{A(IS_{(2)})}$, iterating $i = i + 1$:

(1) Search $\max S_{A(IS_{(x)})}$, store into ${}^{\Delta}\mathbf{S}_{A(1)}$;

(2) Search $\max S_{A(IS_{(x)})}$, store into ${}^{\Delta}\mathbf{S}_{A(2)}$;

Step 2.2: Add $S_{A(IS_{(3)})}$. Compare $S_{A(IS_{(1)})}$, $S_{A(IS_{(2)})}$, and $S_{A(IS_{(3)})}$, iterating $i = i + 1$:

(1) Search $\max S_{A(IS_{(x)})}$, store into ${}^{\Delta}\mathbf{S}_{A(1)}$;

(2) Search $sub\max S_{A(IS_{(x)})}$ and store into ${}^{\Delta}\mathbf{S}_{A(2)}$;

(3) Search $\max S_{A(IS_{(x)})}$, store into ${}^{\Delta}\mathbf{S}_{A(3)}$.

Step 2.3: Add the $S_{A(IS_{(i)})}$, traversing $i \in (3, \max i]$, in line with the same algorithm from Step 2.1 to Step 2.2, compare $S_{A(IS_{(1)})}$, $S_{A(IS_{(2)})}$, …, $S_{A(IS_{(i)})}$. Descend to store $S_{A(IS_{(i)})}$ into ${}^{\Delta}\mathbf{S}_A$, iterating $i = i + 1$.

Step 2.4: Loop iteration $i = i + 1$ until $i = k$, iteration ends. Output a full ranked vector $i = k$. Take the seed point $s_{eed(i)} \sim IS_{(i)}$ of the current element ${}^{\Delta}\mathbf{S}_{A(1)}$ as the cluster $C_{(i,1)}$ seed point where the POI $P_{(1)}$ is located. Store $S_{A(IS_{(i)},P_{(1)})}$ into element $S_{A(i,1)}$ of matrix ${\mathbf{S}_{A(i,j)}}^*$, note $P_{(1)} \in C_{(i)}$.

Step 3: For g number of POIs $P_{(i)}$, take $i = 2$ and calculate the $S_{A(IS_{(i)},P_{(2)})}$ between $P_{(2)}$ and k number of the seed points $s_{eed(i)}$. According to the Step 2 algorithm, iterate $i = i + 1$ and store $S_{A(IS_{(i)})}$ in ${}^{\Delta}\mathbf{S}_A$ by descending order. At the end of the iteration $i = k$, output a full ranked vector ${}^{\Delta}\mathbf{S}_A$. Take the seed point $seed(i) \sim IS_{(i)}$ of the current element ${}^{\Delta}\mathbf{S}_{A(1)}$ as the cluster $C_{(i,1)}$ seed point where the POI $P_{(2)}$ is located. Store $S_{A(IS_{(i)},P_{(2)})}$ into element $S_{A(i,j)}$ of matrix ${\mathbf{S}_{A(i,j)}}^*$, note $P_{(2)} \in C_{(i)}$.

Step 4: As to the g number of POIs $P_{(i)}$, iterating $i = i + 1$, and traversing $i \in (0, g]$. When a $P_{(i)}$ is iterated, store $S_{A(IS_{(i)},P_{(i)})}$ into element $S_{A(i,j)}$ of matrix ${\mathbf{S}_{A(i,j)}}^*$, note $P_{(i)} \in C_{(i)}$.

Step 5: As to the $P_{(i)}$, until the $i = g$ is iterated. Output the full ranked matrix ${\mathbf{S}_{A(i,j)}}^*$, the algorithm ends.

3.1.3. POI Recommendation Algorithm Based on Attribute Weight for ICV Navigation Route

Considering the different preference degrees of the tourists to the POI feature attributes and spatial attributes, we introduce the concept of attribute to determine the preferences of tourists to the POI feature attributes and spatial attributes [19,20]. The key elements in constructing the ICV optimal POI recommendation algorithm are as follows. In the algorithm, the attribute weight factor and POI recommendation degree are the two most importation attributes.

(1) The matching between the POI feature attributes and the tourists' interests, i.e., feature attribute recommendation degree $\zeta(\mathbf{f}_{T(i)}, \mathbf{f}_{P(i)})$;

(2) When the ICV travels on the tour route, considering the urgent situations such as power outages, sudden malfunctions, traffic accidents, tourist suspensions and adverse weather conditions, the ICV tour route should surround the ICV transfer stations $IS_{(i)}$ and search for the POIs with the best spatial accessibility $S_{A(IS_{(i)},P_{(i)})}$ within the cluster $C_{(i)}$ including $IS_{(i)}$.

(3) The setting of attribute weight should balance $\zeta(\mathbf{f}_{T(i)}, \mathbf{f}_{P(i)})$ and $S_{A(IS_{(i)},P_{(i)})}$.

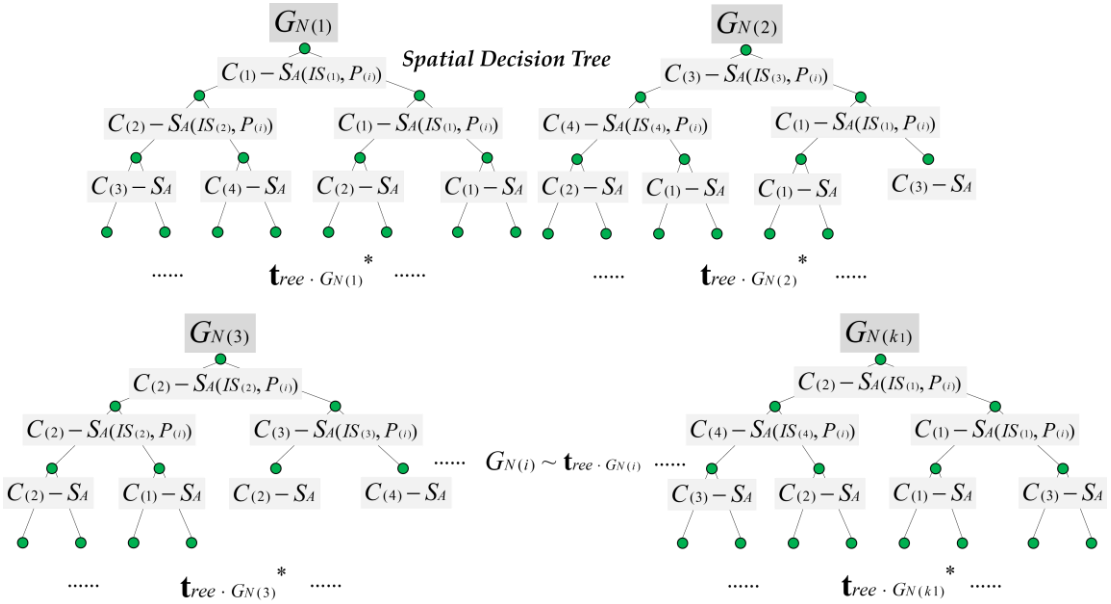

Figure 6. The topological forest with the labeled spatial accessibility based on the decision forest. The node "*" means the improved decision tree with the cluster and the spatial accessibility.

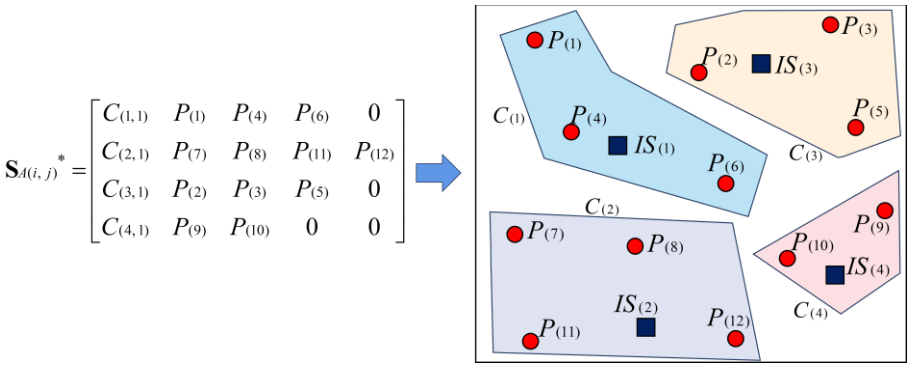

Figure 7. An example of POI spatial cluster constructed by matrix $\mathbf{S}_{A(i,j)}^{*}$.

For the balancing on tourists' interests, we set two factors $\varepsilon_{(1)}$ and $\varepsilon_{(2)}$ to constrain the tourists' preferences to the POI feature attributes and spatial attributes, and specify that $0 < \varepsilon_{(i)} < 1, i \in [1,2], i \in \mathbf{N}, \varepsilon_{(i)} \in \mathbf{R}$, the $\varepsilon_{(1)}$ and $\varepsilon_{(2)}$ must satisfy the Formula (11). The POI recommendation degree $\zeta_{P_{(i)}}$ for constructing the ICV navigation route is shown in Formula (12).

$$\varepsilon_{(1)} + \varepsilon_{(2)} = 1 \tag{11}$$

$$\zeta_{P_{(i)}} = \varepsilon_{(1)} \cdot \zeta(\mathbf{f}_{T(i)}, \mathbf{f}_{P(i)}) + \varepsilon_{(2)} \cdot S_{A(IS_{(i)}, P_{(i)})} \tag{12}$$

Based on the idea and method of recommending POIs for ICVs, we construct the optimal POI recommendation algorithm based on attribute weight for tourism ICVs as follows (Algorithm 3). Figure 8 is a schematic diagram of the process for constructing the optimal POI recommendation algorithm:

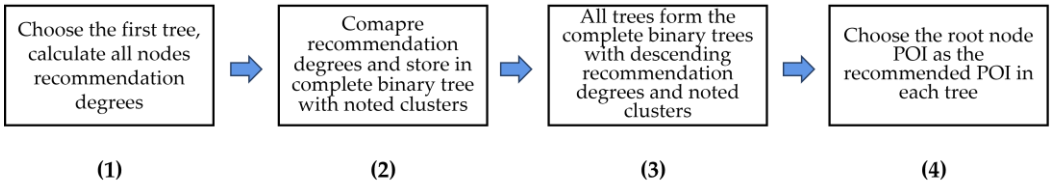

Figure 8. The process for constructing the optimal POI recommendation algorithm.

Subfigure (1) shows the first step of the algorithm: selecting the first decision tree and calculating the recommendation degrees $\zeta_{P_{(i)}}$ of POIs for all nodes;

Subfigure (2) shows the second step of the algorithm: comparing the recommendation degrees of $N_{ode(1,1)}$ and $N_{ode(2,1)}$ with the larger value stored at the root node and the smaller value stored at the left child node of the lower level; Comparing the recommendation degrees of $N_{ode(1,1)}$, $N_{ode(2,1)}$ and $N_{ode(2,2)}$ with the maximum value stored at the root node, the larger value stored at the left child node of the lower level, and the minimum value stored at the right child node of the lower level; and so on. All POI recommendation degrees are finally stored and the corresponding clusters for all nodes are marked;

Subfigure (3) shows the third step of the algorithm: generating a recommendation degree heap sorting structure for all the decision trees and labeling the clusters;

Subfigure (4) shows the fourth step of the algorithm: selecting the optimal POI corresponding to the root node of each decision tree.

Algorithm 3: The optimal POI recommendation algorithm based on the attribute weight for tourism ICVs

Input: Spatial topological forest $\mathbf{f}_{orest \cdot G_{N(i)}}{}^{*}$, attribute weight factor $\varepsilon_{(i)}$

Output: The best matched POIs $P_{(i)}$ for tourists' interests.

Step 1: Select decision tree $\mathbf{t}_{ree \cdot G_{N(i)}}{}^{*}$ of the decision forest $\mathbf{f}_{orest \cdot G_{N(i)}}{}^{*}$. Calculate POI recommendation degrees $\zeta_{P_{(i)}}$ for all nodes in the decision tree.

Step 2: Construct the optimization algorithm for the maximum heap sorting decision tree $\mathbf{t}_{ree \cdot G_{N(1)}}{}^{*}$.

Step 2.1: Compare the root node $N_{ode(1,1)}$ with the child node $N_{ode(2,1)}$ in recommendation degree $\zeta P_{(i)} \sim \zeta N_{ode(x,y)}$:

(1) If $\zeta N_{ode(1,1)} \geq \zeta N_{ode(2,1)}$, keep the storage unchanged;

(2) If $\zeta N_{ode(1,1)} < \zeta N_{ode(2,1)}$, store $\zeta N_{ode(1,1)}$ and $\zeta N_{ode(2,1)}$ into $N_{ode(2,1)}$ and $N_{ode(1,1)}$.

Step 2.2: Add the child node $N_{ode(2,2)}$, compare $N_{ode(1,1)}$, $N_{ode(2,1)}$, and $N_{ode(2,2)}$ in recommendation degree $\zeta N_{ode(1,1)}$, $\zeta N_{ode(2,1)}$, and $\zeta N_{ode(2,2)}$.

(1) Store $\max\left(\zeta N_{ode(1,1)}, \zeta N_{ode(2,1)}, \zeta N_{ode(2,2)}\right)$ into root node $N_{ode(1,1)}$;

(2) Store $\min\left(\zeta N_{ode(1,1)}, \zeta N_{ode(2,1)}, \zeta N_{ode(2,2)}\right)$ into child node $N_{ode(2,2)}$;

(3) Store the remaining recommendation degree into $N_{ode(2,1)}$.

Step 2.3: In line with the same algorithm from Step 2.1 to Step 2.2, store the recommendation degrees $\zeta P_{(i)} \sim \zeta N_{ode(x,y)}$ in descending order, so that the recommendation degree $\zeta_{P_{(i)}}$ of any No. α layer in the decision tree $\mathbf{t}_{ree \cdot G_{N(i)}}{}^{*}$ is always greater than recommendation degree $\zeta_{P_{(i)}}$ in the next No. $\alpha + 1$ layer. At the same time, the recommendation degree of the left node $N_{ode(\alpha,y)}$ in any No. α layer is always greater than that of any right node $N_{ode(\alpha,y+\Delta\omega)}$, in which $\Delta\omega$ is a slight increase that meets $\beta + \Delta\omega \leq k_{N_{ode(i)}}$ and $k_{N_{ode(i)}}$ is the number of nodes in the No. n layer.

Step 2.4: Mark the cluster $C_{(i)}$ which the current recommendation degree of each node belongs to, and the optimization algorithm for the decision tree $\mathbf{t}_{ree \cdot G_{N(1)}}{}^{*}$ ends.

Step 3: Select decision tree $\mathbf{t}_{ree \cdot G_{N(i)}}{}^{*}$ of the decision forest $\mathbf{f}_{orest \cdot G_{N(i)}}{}^{*}$. Calculate POI recommendation degrees $\zeta_{P_{(i)}}$ for all nodes in the decision tree. In line with the algorithm in Step 2, realize the optimization for $\mathbf{t}_{ree \cdot G_{N(i)}}{}^{*}$. Traversing $i \in (1, \max i]$.

Step 4: As to $\mathbf{t}_{ree \cdot G_{N(i)}}{}^{*}$, until the $i = k_1$ is iterated. The optimization algorithm for the decision forest $\mathbf{f}_{orest \cdot G_{N(i)}}{}^{*}$ ends. Output the optimal POIs $P_{(i)}$ in each decision tree $\mathbf{t}_{ree \cdot G_{N(i)}}{}^{*}$, relating clusters $C_{(i)}$, and ICV transfer stations $IS_{(i)}$.

3.2. Tourism ICV Navigation Route Model Based on the Improved Fruit Fly Optimization Algorithm

During the ICV route-searching and selection process, the movement of ICVs between different POIs will produce the time costs, which are directly related to the distance of ICV movement. Firstly, the spatial accessibility generated by the locations of the ICV and the POI determines the spatial cost. The larger the spatial accessibility is, the lower the time and distance costs for the ICV to move from its current location to the POI will be. The smaller the spatial accessibility is, the greater the time and distance costs for the ICV to move from its current location to the POI will be. Therefore, when constructing an ICV navigation route model, the spatial accessibility between ICV and POI, as well as the resulting movement time and distance, are the key factors determining the quality of ICV navigation routes and are the core elements for constructing the optimal ICV navigation route model. In the process of constructing the improved fruit fly optimization algorithm to search for the optimal routes, the road nodes and node path distances relating to the urban geospatial constraints are involved. As no toll is charged for any vehicle passing on the urban public open roads, i.e., there is no toll on the urban roads, the algorithm construction does not consider the road toll.

The fruit fly optimization algorithm is a designed bionic algorithm to simulate the foraging behavior of fruit flies. Its principle and calculation process are simple and easy to implement. The basic principle is to simulate the process of fruit flies continuously approaching food and ultimately finding the food, which has the characteristics of random direction, random step size, and group convergence, and can ultimately find the global optimal solution [21,22]. The reasons for choosing the fruit fly optimization algorithm to search for the optimal ICV guidance route are as follows:

(1) The searching for the route nodes has the feature of arbitrariness. When an ICV leaves a node to search for the next node, it has the feature of randomness in point selection, which is consistent with the characteristic of random searching by fruit flies;
(2) The searching direction has the feature of arbitrariness. When an ICV leaves a node to search for the next node, it has directional randomness, which is consistent with the characteristic of random searching by fruit flies;
(3) When an ICV selects a path node, randomly selecting the next node is equivalent to replacing a target node, which is related to changing a step size, and identical to the principle of the fruit fly optimization algorithm's step-size searching.
(4) The fruit fly optimization algorithm has the characteristic of population convergence. After each searching cycle, all the fruit flies fly towards the current optimal solution. During the searching process, individuals which are not the optimal solution can be excluded, and the convergence speed is fast.

In this section, we construct an improved fruit fly optimization algorithm. Firstly, we use the recommended POIs as the ICV navigation route nodes to construct a fruit fly optimization sub-interval, and use the road nodes within the sub-interval as the ICV sub-interval passing nodes to construct the fruit fly individuals. Secondly, we take the ICV transfer stations $IS_{(i)}$, where tourists take the ICVs and depart from, as the starting points of the ICV navigation routes, and the ICV transfer stations $IS_{(i)}$, where tourists ultimately return the ICVs, as the ending points of the ICV navigation routes. The POIs with the highest recommendation degrees $\zeta_{P_{(i)}}$ within the cluster $C_{(i)}$ corresponding to each transfer station $IS_{(i)}$ are the POIs to be visited. They are used to construct the optimal ICV guidance route. ICVs move within the sub-intervals in a unidirectional way, meaning that they move from one POI to another without following a repetitive or turnaround route. Based on the analysis, combined with the decision results of the ICV on POIs and the travel mode of ICV navigation routes, the problem of searching for the optimal ICV navigation route is transformed into constructing the fruit fly individuals in each sub-interval and searching for the optimal navigation route in each sub-interval. The global optimal ICV navigation route is obtained by iterating the optimal routes from all the sub-intervals. In

the algorithm, the fruit fly individual in sub-interval, mileage cost function, and odor concentration function are the three most important attributes.

Compared to the traditional fruit fly optimization algorithm in searching for the optimal solution, our proposed improved fruit fly optimization algorithm better conforms to ICV decision-making logic and travel mode, resulting in significant improvement. Firstly, the traditional fruit fly optimization algorithm uses the spatial location as a criterion for initializing the fruit fly individuals, while our proposed improved optimization algorithm uses tour route cost as a criterion, which is aimed at the optimization and improvement of specific applications. Secondly, the traditional fruit fly optimization algorithm compares the odor concentrations between fruit fly individuals while randomly searching for the individuals. It requires prior determination of the number of individuals, iteration times, and food location, etc. The iterative process is relatively complex and has high time complexity. Our proposed improved fruit fly optimization algorithm traverses all fruit fly individuals, and initially determines the fruit fly population with the odor concentration to be compared, and then converts them all into pathways between POIs. Then, through the step size transformation for comparison, it reduces the structural and time complexity of the algorithm, improves the readability of the pseudocode, and makes significant progress compared to the traditional fruit fly optimization algorithm. Thirdly, the traditional fruit fly optimization algorithm sets a random step size when individuals fly and search for food, which has significant blindness. However, our proposed improved algorithm is based on the 2-opt transformation of road nodes. Due to the fixed distance between road nodes, the fruit fly step size has precise quantitative values, and the calculation steps and results are more accurate.

Definition 1. *ICV navigation route sub-interval $R_{sub(i)}$ and sub-interval nodes $n_{sub(i)}$. The ICV path formed between the transfer station $IS_{(i)}$ and POI $P_{(i)}$ or between POI $P_{(i)}$ and POI $P_{(j)}$ on the ICV tour route is defined as the ICV navigation route sub-interval, denoted as $R_{sub(i)}$. The road nodes that ICV passes through during one-way movement within a sub-interval $R_{sub(i)}$ are defined as sub-interval nodes, denoted as $n_{sub(i)}$. Set the number of nodes $n_{sub(i)}$ included in a sub-interval as $k_{sub(i)}$.*

Definition 2. *Fruit fly solution space $\mathbf{F}_{R_{sub(i)}}$ and fruit fly individual $f_{R_{sub(i,j)}}$ based on sub-interval $R_{sub(i)}$. Within a sub-interval $R_{sub(i)}$, the ICV moves from the starting point $IS_{(i)}$ or $P_{(i)}$; avoiding repeating or turning back, it passes through several nodes $n_{sub(i)}$ and moves to the terminal point $P_{(j)}$ of the sub-interval, and the whole process forms an ICV travel pathway; this pathway is defined as a fruit fly individual, denoted as $f_{R_{sub(i,j)}}$, in which i represents the sub-interval number and j represents the fruit fly individual number. In a sub-interval $R_{sub(i)}$, the solution set composed of all fruit fly individuals $f_{R_{sub(i,j)}}$ is defined as the fruit fly solution space $\mathbf{F}_{R_{sub(i)}}$.*

The quantity of the feasible solutions in the solution space $\mathbf{F}_{R_{sub(i)}}$ is determined by the maximum number of footmarks for the individual fruit flies $f_{R_{sub(i,j)}}$. The locations of the $k_{sub(i)}$ number of nodes $n_{sub(i)}$ in $R_{sub(i)}$ are fixed. In a sub-interval, the ICV moves in a unidirectional way and traverses limited nodes $n_{sub(i)}$. According to the definition, a fruit fly individual $f_{R_{sub(i,j)}}$ relates to a $1 \times \left(p_{sub(i)} + 2\right)$ dimensional vector $\mathbf{f}_{R_{sub(i,j)}}$ composed of $p_{sub(i)}$ number of nodes $n_{sub(i)}$ passed by an ICV. The first element of the vector is the starting point $IS_{(i)}$ or $P_{(i)}$ of the sub-interval $R_{sub(i)}$, and the last element is the terminal point $P_{(j)}$ or $IS_{(j)}$ of sub-interval $R_{sub(i)}$, satisfying $0 < p_{sub(i)} < k_{sub(i)}$, $p_{sub(i)}, k_{sub(i)} \in \mathbf{N}$. The elements contained in the vector $\mathbf{f}_{R_{sub(i,j)}}$ corresponding to the individual fruit flies $f_{R_{sub(i,j)}}$ are $f_{R_{sub(i,j,t)}}$, in which i represents the sub-interval number, j represents the individual fruit fly number, and t represents one node $n_{sub(i)}$ within $\mathbf{f}_{R_{sub(i,j)}}$.

According to the definition, the modeling steps and preset constraints for constructing an individual fruit fly $f_{R_{sub(i,j)}}$ are as follows (starting from a POI):

(1) Initialize the sub-interval $R_{sub(i)}$, including $k_{sub(i)} = 12$ number of nodes $n_{sub(i)}$, starting point $P_{(i)}$, and and terminal point $P_{(j)}$, as shown in the Figure 9(1).
(2) Step 1: Select $n_{sub(1)}$ or $n_{sub(2)}$. Node $n_{sub(1)}$ is found, then a feasible path is formed, keep $n_{sub(1)}$, as shown in the Figure 9(2).
(3) Step 2: Select $n_{sub(3)}$ or $n_{sub(4)}$. Node $n_{sub(4)}$ is found, then a feasible path is formed, keep $n_{sub(4)}$, as shown in the Figure 9(3).
(4) Step 3: Select $n_{sub(5)}$, $n_{sub(6)}$, or $n_{sub(7)}$. Node $n_{sub(7)}$ is found, then a feasible path is formed, keep $n_{sub(7)}$, as shown in the Figure 9(4).
(5) Step 4: Select $n_{sub(8)}$ or $n_{sub(11)}$. Node $n_{sub(11)}$ is found, then a feasible path is formed, keep $n_{sub(11)}$, as shown in the Figure 9(5).
(6) Step 5: Select $n_{sub(9)}$ or $n_{sub(10)}$. Node $n_{sub(10)}$ is found, then a feasible path is formed, keep $n_{sub(10)}$, as shown in the Figure 9(6).
(7) Step 6: Node $n_{sub(12)}$ is found, then a feasible path is formed, keep $n_{sub(12)}$, as shown in the Figure 9(7).
(8) Step 7: Arrive at the POI $P_{(j)}$ and form a pathway $n_{sub(i)} \rightarrow 1, 4, 7, 11, 10, 12$, which constitutes one individual fruit fly $f_{R_{sub(i,j)}}$, as shown in the Figure 9(8). The searching process ends.

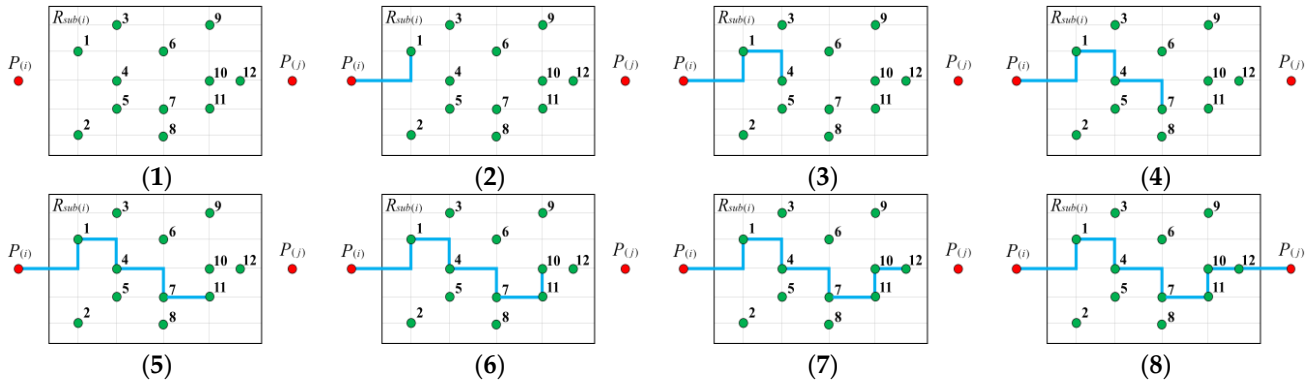

Figure 9. The process of searching for fruit fly individuals. Each subfigure shows one step of the searching process. The number in the figure represents the road node number.

Definition 3. *The current optimal solution* $f_{R_{sub(i,j)}}{}^{\Delta}$ *in solution space* $\mathbf{F}_{R_{sub(i)}}$. *The optimal solution found by the fruit fly group during the search for food in the solution space* $\mathbf{F}_{R_{sub(i)}}$ *is defined as the current optimal solution* $f_{R_{sub(i,j)}}{}^{\Delta}$ *in the solution space.*

The purpose of establishing the current optimal solution mechanism in the solution space is to ensure that the fruit flies $f_{R_{sub(i,j)}}$ always fly towards the current optimal solution $f_{R_{sub(i,j)}}{}^{\Delta}$ when searching for the global optimal solution, and to preserve the current optimal solution. When a better fruit fly individual is found, the current optimal solution will be replaced to ensure that the algorithm does not fall into the local optimal solution.

Definition 4. *Fruit fly step size* $L_{e(t1,t2)}$. *The fruit fly group always searches for food in a certain direction; that is, flying towards the fruit fly with the highest odor concentration, and the flight follows a certain regular pattern. For an individual fruit fly* $f_{R_{sub(i,j)}}$, *define the fly step size* $L_{e(t1,t2)}$ *as a 2-opt operation between arbitrary element* $\forall f_{R_{sub(i,j,t1)}}$ *and* $\forall f_{R_{sub(i,j,t2)}}$ *in the vector* $\mathbf{f}_{R_{sub(i,j)}}$.

According to the definition, individual fruit fly $f_{R_{sub(i,j)}}$ must go several steps $L_{e(t1,t2)}$ towards the fruit fly $f_{R_{sub(i,j)}}{}^{\Delta}$ with the highest odor concentration. We construct a flying

distance model $L(f_{R_{sub(i,j)}}, f_{R_{sub(i,j)}}{}^{\Delta})$ for individual fruit fly $f_{R_{sub(i,j)}}$ as shown in Formula (13), and then an iterating model $f_{R_{sub(i,j)}}{}^{\Delta}$ is constructed as shown in Formula (14).

$$L(f_{R_{sub(i,j)}}, f_{R_{sub(i,j)}}{}^{\Delta}) = \sum_{u=1}^{\max u} L_{e(t1_{(u)}, t2_{(u)})} \tag{13}$$

$$f_{R_{sub(i,j)}}{}^{\Delta} = f_{R_{sub(i,j)}} + \sum_{u=1}^{\max u} L_{e(t1_{(u)}, t2_{(u)})}. \tag{14}$$

Definition 5. *Distance cost function $S(f_{R_{sub(i,j)}})$ and odor concentration function $O(f_{R_{sub(i,j)}})$. The criterion for determining whether an individual fruit fly $f_{R_{sub(i,j)}}$ is a fruit fly $f_{R_{sub(i,j)}}{}^{\Delta}$ is the concentration of food odor in the $f_{R_{sub(i,j)}}$ location. In the ICV navigation route-searching process, the ICV starts from the starting point and travels along the path represented by the vector $\boldsymbol{f}_{R_{sub(i,j)}}$ corresponding to one fruit fly $f_{R_{sub(i,j)}}$ in the sub-interval $R_{sub(i)}$, and ultimately reaches the terminal point. The distance traveled by the ICV during this process is defined as the distance cost function, denoted as $S(f_{R_{sub(i,j)}})$. According to the definition, the distance cost function of the fruit fly is formed by the iteration of distances between nodes $n_{sub(i)}$ in vector $\boldsymbol{f}_{R_{sub(i,j)}}$. The function that uses the distance cost function $S(f_{R_{sub(i,j)}})$ to determine whether a fruit fly individual is the current optimal individual $f_{R_{sub(i,j)}}{}^{\Delta}$ is defined as the odor concentration function, denoted as $O(f_{R_{sub(i,j)}})$.*

The distance cost function $O(f_{R_{sub(i,j)}})$ and odor concentration function $O(f_{R_{sub(i,j)}})$ we construct are shown in the Formulas (15) and (16).

$$\begin{aligned} S(f_{R_{sub(i,j)}}) = \; & d(P_{(i)}, f_{R_{sub(i,j,t)}}) + d(f_{R_{sub(i,j,psub(i))}}, P_{(j)}) \\ & + \sum_{t=1}^{psub(i)-1} d(f_{R_{sub(i,j,t)}}, f_{R_{sub(i,j,t+1)}}) \end{aligned} \tag{15}$$

$$O(f_{R_{sub(i,j)}}) = \frac{1}{S(f_{R_{sub(i,j)}})} \tag{16}$$

According to the definition and algorithm idea, the searched global optimal solution for the fruit fly group within the sub-interval $R_{sub(i)}$ is the shortest path between $P_{(i)}$ and $P_{(j)}$, which corresponds to the fruit fly individual $f_{R_{sub(i,j)}}$ with the maximum odor concentration function value $O(f_{R_{sub(i,j)}})$. We propose to construct an ICV navigation route model based on an improved fruit fly optimization algorithm. The basic idea is: determine the initial positions of all the fruit fly individuals $f_{R_{sub(i,j)}}$ in the sub-interval $R_{sub(i)}$ solution space $\mathbf{F}_{R_{sub(i,j)}}$, and randomly select the fruit fly individual $randf_{R_{sub(i,j)}}$ as the current optimal solution $f_{R_{sub(i,j)}}{}^{\Delta}$. All fruit flies fly to $randf_{R_{sub(i,j)}}$ with the step $L_{e(t1,t2)}$, and when a unit step $L_{e(t1,t2)}$ is iterated, the algorithm judges the current state of the fruit fly group to determine whether any fruit fly individual has a higher odor concentration than $randf_{R_{sub(i,j)}}$, and then decides whether to perform the replacement operation. With the new current optimal solution $f_{R_{sub(i,j)}}{}^{\Delta}$ as the goal, all fruit flies fly towards it and repeat the above searching steps until the fruit fly individual with the highest odor concentration $O(f_{R_{sub(i,j)}})$ is found. The following is the constructed tourism ICV navigation route model based on the improved fruit fly optimization algorithm (Algorithm 4), and Figure 10 shows the process of searching for the global optimal ICV navigation route by using the improved fruit fly optimization algorithm. Within the figure,

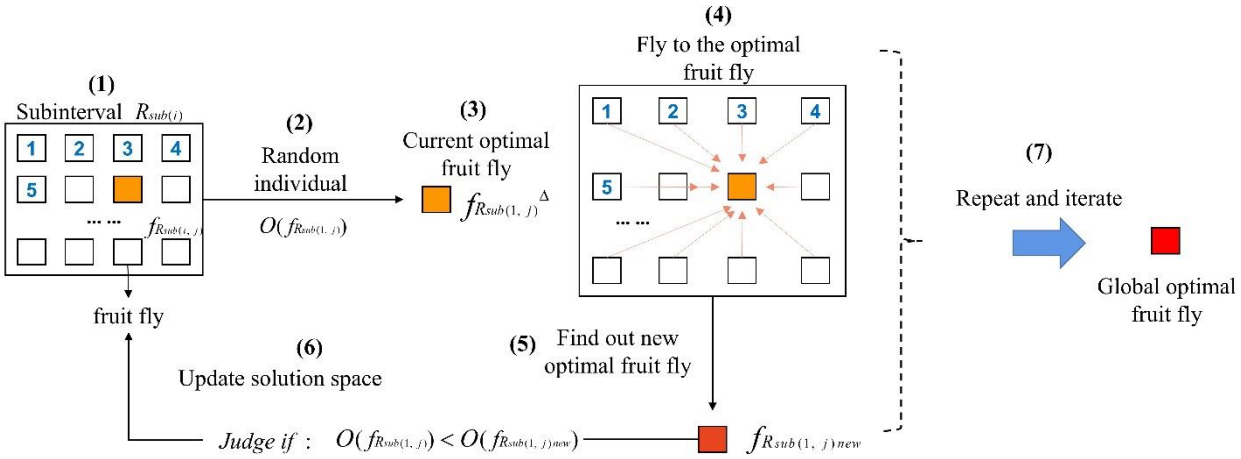

Figure 10. The process of searching for the global optimal ICV navigation route by the improved fruit fly optimization algorithm.

Subfigure (1) represents constructing the sub-intervals between ICV and POI, or between two POIs. The sub-intervals are denoted as 1, 2, 3,. . .;

Subfigure (2) represents randomly choosing the pathway represented by one fruit fly individual from the sub-interval;

Subfigure (3) represents supposing the randomly selected fruit fly individual as the optimal individual, representing the current location of the food;

Subfigure (4) represents all the fruit fly individuals in the sub-interval flying towards the current optimal fruit fly individual by the step size, generating a new optimal individual during the flying process;

Subfigure (5) represents the optimal fruit fly individual produced during the flying process;

Subfigure (6) represents determining whether its odor concentration is greater than the current optimal fruit fly individual, and performing a replacement operation; Return to subgraph (1) to generate a new subinterval state;

Subfigure (7) represents continuing to iterate the new optimal fruit fly individual until the globally optimal fruit fly individual within the sub-interval is found.

Algorithm 4: Tourism ICV navigation route model based on the improved fruit fly optimization algorithm

Input: Recommended POI, sub-interval $R_{sub(i)}$, node $n_{sub(i)}$ for each sub-interval, starting point $IS_{(i)}$ or $P_{(i)}$, terminal point $IS_{(j)}$ or $P_{(j)}$.

Output: Optimal ICV navigation route

Step 1: As to the sub-interval $R_{sub(i)}$, take $i = 1$, construct the optimal ICV route for the first sub-interval.

Step 1.1: Initialize the fruit fly individual $f_{R_{sub(1,j)}}$ and solution space $\mathbf{F}_{R_{sub(1)}}$.

Step 1.2: Set up the sub-interval model $R_{sub(1)}$. Confirm the starting point $IS_{(i)}$, node $n_{sub(i)}$, terminal point $P_{(i)}$;

Step 1.3: Starting point $IS_{(i)}$ of $R_{sub(1)}$ searches for node $n_{sub(1)}$. Judge whether there exists a $\neg n_{sub(1)}$ that will be absorbed into $f_{R_{sub(1,j)}}$ in $R_{sub(1)}$:

(1) Exists: Add it into element $f_{R_{sub(1,1,t)}}$ of $f_{R_{sub(1,1)}}$. Continue to judge whether there exists $\neg n_{sub(1)}$, until the terminal point $P_{(i)}$ is searched, which forms a complete $f_{R_{sub(1,1)}}$. Output vector $\mathbf{f}_{R_{sub(1,1)}}$;

(2) Does not exist: turn to Step 1.4 and search $f_{R_{sub(1,2)}}$.

Algorithm 4: *Cont.*

Step 1.4: Starting point $IS_{(i)}$ of $R_{sub(1)}$ searches for node $n_{sub(2)}$. Judge whether there exists a $\neg n_{sub(2)}$ that will be absorbed into $f_{R_{sub(1,j)}}$ in $R_{sub(1)}$:

(1) Exists: Add it into element $f_{R_{sub(1,2,t)}}$ of $f_{R_{sub(1,2)}}$. Continue to judge whether there exists $\neg n_{sub(2)}$, until the terminal point $P_{(i)}$ is searched, which forms a complete $f_{R_{sub(1,2)}}$. Output vector $\mathbf{f}_{R_{sub(1,2)}}$;

(2) Does not exist: turn to Step 1.5 and search $\mathbf{f}_{R_{sub(1,3)}}$.

Step 1.5: Starting point $IS_{(i)}$ of $R_{sub(1)}$ searches for node $n_{sub(i)}$. Judge whether there exists a $\neg n_{sub(i)}$ that will be absorbed into $f_{R_{sub(1,j)}}$ in $R_{sub(1)}$:

(1) Exists: Add it into element $f_{R_{sub(1,j,t)}}$ of $f_{R_{sub(1,j)}}$. Continue to judge whether there exists $\neg n_{sub(i)}$, until the terminal point $P_{(i)}$ is searched, which forms a complete $f_{R_{sub(1,j)}}$. Output vector $\mathbf{f}_{R_{sub(1,j)}}$. This process traverses $j \in (2, \lambda_1]$, and the searching ends. Turn to Step 1.6.

(2) Traverse $j \in (2, \lambda_1]$, if $\neg n_{sub(i)}$ still does not exist, then the sub-interval $R_{sub(1)}$ does not exist. The searching ends, turn to Step 1.6.

Step 1.6: Output the solution space $\mathbf{F}_{R_{sub(1)}}$, including λ_1 number of fruit fly individual $f_{R_{sub(1,j)}}$, namely max$j = \lambda_1$.

Step 2: In line with the same algorithm as Step 1, as to the sub-interval $R_{sub(i)}$, take $i = 2$, construct the optimal ICV route for the second sub-interval. Output solution space $\mathbf{F}_{R_{sub(2)}}$, including λ_2 number of fruit fly individuals $f_{R_{sub(1,j)}}$, namely max$j = \lambda_2$.

Step 3: Continue searching, and output solution space $\mathbf{F}_{R_{sub(i)}}$, including λ_i number of fruit fly individuals $f_{R_{sub(1,j)}}$, namely max$j = \lambda_i$. Traverse solution space $\mathbf{F}_{R_{sub(i)}}$, corresponding to $i \in (2, \max i]$. Output all fruit fly individuals $f_{R_{sub(i,j)}}$ for all sub-intervals $R_{sub(i)}$ in ICV navigation route.

Step 4: Update locations in the fruit fly group $\mathbf{F}_{R_{sub(1)}}$. Iterate to calculate the optimal fruit fly individual ${f_{R_{sub(1,j)}}}^{\Delta}$ for $R_{sub(1)}$. Output the optimal navigation route for $R_{sub(1)}$.

Step 4.1: Randomly select a fruit fly individual $rand f_{R_{sub(1,j)}}$ as ${f_{R_{sub(1,j)}}}^{\Delta}$, calculate $O(f_{R_{sub(1,j)}})$;

Step 4.2: As to $\forall f_{(1,\neg j)}$, fly to $f_{R_{sub(1,j)}}$ by unit step size $L_{e(t1,t2)}$. Update locations in the fruit fly group $\mathbf{F}_{R_{sub(1)}}$. Set that after flying by unit step size, $\forall f_{(1,\neg j)}$ turns to $f_{R_{sub(1,j)new}}$, make judgement:

(1) If $O(f_{R_{sub(1,j)}}) > O(f_{R_{sub(1,j)new}})$, keep current $f_{R_{sub(1,j)}}$ as ${f_{R_{sub(1,j)}}}^{\Delta}$, and all fruit flies continue flying to $f_{R_{sub(1,j)}}$ with step size $L_{e(t1,t2)}$, turn to Step 4.3 and judge $f_{R_{sub(1,j)new}}$;

(2) If there exists $\forall f_{R_{sub(1,j)new}}$ that makes $O(f_{R_{sub(1,j)}}) < O(f_{R_{sub(1,j)new}})$, replace ${f_{R_{sub(1,j)}}}^{\Delta}$ with $f_{R_{sub(1,j)new}}$, turn to Step 4.3 and continue searching.

Step 4.3: Based on current ${f_{R_{sub(1,j)}}}^{\Delta}$, fly to ${f_{R_{sub(1,j)}}}^{\Delta}$ by unit step size $L_{e(t1,t2)}$. Update locations in the fruit fly group $\mathbf{F}_{R_{sub(1)}}$. Make judgement:

(1) If $O({f_{R_{sub(1,j)}}}^{\Delta}) > O(f_{R_{sub(1,j)new}})$, keep ${f_{R_{sub(1,j)}}}^{\Delta}$ as current solution, and all fruit flies continue flying to ${f_{R_{sub(1,j)}}}^{\Delta}$ with step size $L_{e(t1,t2)}$, turn to Step 4.4 and judge $f_{R_{sub(1,j)new}}$;

(2) If there exists $\forall f_{R_{sub(1,j)new}}$ that makes $O({f_{R_{sub(1,j)}}}^{\Delta}) < O(f_{R_{sub(1,j)new}})$, replace ${f_{R_{sub(1,j)}}}^{\Delta}$ with $f_{R_{sub(1,j)new}}$, turn to Step 4.4 and continue searching.

Step 4.4: Repeat Step 4.1 to Step 4.3. Update locations in the fruit fly group $\mathbf{F}_{R_{sub(1)}}$ until a certain $f_{R_{sub(1,j)new}}$ is searched as the global optimal solution in solution space $\mathbf{F}_{R_{sub(1)}}$, relating to the optimal function value $O(f_{R_{sub(1,j)}})_{opt}$, and its vector $f_{R_{sub(1,j)new}} \sim \mathbf{f}_{R_{sub(1,j)}}$ relates to the optimal ICV navigation route in $R_{sub(1)}$.

Step 5: Update locations in the fruit fly group $\mathbf{F}_{R_{sub(2)}}$, iterate to calculate the optimal fruit fly ${f_{R_{sub(2,j)}}}^{\Delta}$ in $R_{sub(2)}$, and output the optimal ICV navigation route in $R_{sub(2)}$.

Step 6: Update locations in the fruit fly group $\mathbf{F}_{R_{sub(i)}}$, iterate to calculate the optimal fruit fly ${f_{R_{sub(i,j)}}}^{\Delta}$ in $R_{sub(i)}$, and output the optimal ICV navigation route in $R_{sub(i)}$, traversing $i \in (2, \max i]$. Output the optimal ICV navigation routes in all sub-intervals $R_{sub(i)}$.

Step 7: Connect all the optimal navigation routes in all $R_{sub(i)}$ from the starting point $IS_{(i)}$ or $P_{(i)}$ to the terminal point $IS_{(j)}$ or $P_{(j)}$, and output the intact optimal ICV navigation route for tourists.

4. Experiment and Result Analysis

4.1. Experimental Objectives

The goal of this section is to design an example experiment to verify the feasibility and accuracy of our proposed algorithm, and to design a comparative experiment to verify the advantages of our proposed algorithm over traditional map route-planning methods and the commonly used shortest route-searching algorithms. The experimental objectives are divided into the following six points:

(1) Goal 1: Test and verify the feasibility and accuracy of POI feature attribute recommendation results;
(2) Goal 2: Test and verify the feasibility and accuracy of the spatial decision forest results;
(3) Goal 3: Verify the feasibility and accuracy of the spatial topology forest results;
(4) Goal 4: Verify the feasibility and accuracy of the recommendation decision forest and the recommended POI output results;
(5) Goal 5: Verify the feasibility and accuracy of the recommended ICV tour route results;
(6) Goal 6: Verify the advantages of the constructed ICV navigation route algorithm over traditional map route-planning methods and the commonly used shortest route-searching algorithms.

4.2. Experiment Process and Data Collection

4.2.1. Experiment Process and Metric Selection

1. Experiment Process

In the experiment, we choose the tourism city Chengdu as the research area, with the representative POIs $P_{(i)}$ within Chengdu as the alternative tourist destinations, and set the ICV transfer stations $IS_{(i)}$ at the main controlling transportation hubs in the downtown area of Chengdu. The main process of the experiment is designed as follows.

(1) Randomly select one tourist as the research subject, determine the natural attributes $G_{N(i)}$ of all the POIs, including: $G_{N(1)}$ "park and green land", $G_{N(2)}$ "cultural and historical commemoration", $G_{N(3)}$ "leisure shopping center", and $G_{N(4)}$ "amusement and theme park". Determine the POI feature attribute vector $\mathbf{f}_{P(i)}$ and the POI feature attribute matrix $\mathbf{f}_{P(i,j)}$, in which the POI feature attributes include $f_{P(1)}$: "travel cost", $f_{P(2)}$: "travel time", $f_{P(3)}$: "POI level (A-Class)", and $f_{P(4)}$: "POI popularity". Determine the tourist interest measurement vector $\mathbf{f}_{T(i)}$ and the tourist interest measurement matrix $\mathbf{f}_{T(i,j)}$ based on the POI feature attributes, then randomly determine and quantify the tourist interest vector, and calculate the POI feature attribute recommendation degree function $\zeta(\mathbf{f}_{T(i)}, \mathbf{f}_{P(i)})$, ultimately generating the spatial decision trees $\mathbf{t}_{ree \cdot G_{N(i)}}$ and the spatial decision forest $\mathbf{f}_{orest \cdot G_{N(i)}}$.
(2) Calculate the POI spatial accessibility $S_{A(IS_{(i)}, P_{(i)})}$ using the spatial relationship between the ICV transfer station $IS_{(i)}$ and the POI $P_{(i)}$, generate the POI spatial clustering matrix $\mathbf{C}_{(i,j)}$, and determine the spatial clustering clusters $C_{(i)}$ with each ICV transfer station $IS_{(i)}$ as the seed point. Generate the topological forest $\mathbf{f}_{orest \cdot G_{N(i)}}{}^{*}$ based on the spatial decision forest $\mathbf{f}_{orest \cdot G_{N(i)}}$ and the spatial clustering $C_{(i)}$ results.
(3) Tourists determine the attribute weight factors $\varepsilon_{(i)}$. Calculate the POI recommendation degree $\zeta_{P_{(i)}}$ based on the topological forest $\mathbf{f}_{orest \cdot G_{N(i)}}{}^{*}$, and output the decision forest $\mathbf{f}_{orest \cdot G_{N(i)}}{}^{*}$ with the labeled spatial clusters $C_{(i)}$ and the recommendation degree $\zeta_{P_{(i)}}$. Determine the optimal POIs recommended to the tourist.
(4) Use the constructed improved fruit fly optimization algorithm to output the optimal ICV navigation routes. Starting from the ICV transfer station $IS_{(i)}$ selected by the tourist, the algorithm searches for the ICV navigation routes one by one through the recommended POIs, and outputs the route with the highest odor concentration function $O(f_{R_{sub(i,j)}})$ in each sub-interval $R_{sub(i)}$. The terminal point of the ICV navigation route is the chosen ICV transfer station $IS_{(i)}$.

(5) The route-searching methods embedded in the Gaode Map (GDM) and the Baidu Map (BDM), and the most representative route-searching algorithms Dijkstra and Floyd–Warshall, are set as the two control groups. Then we design the comparative experiment, in which the proposed algorithm is set as the experimental group, while the map route-planning methods and the commonly used route-searching algorithms are set as the two control groups. We compare the travel costs of our proposed algorithm with the control groups' route-planning methods in outputting the optimal ICV navigation routes.

2. Metric Selection

To verify the advantages of our proposed algorithm comparing to the traditional map algorithms and route-searching algorithms, we design a comparative experiment. The following metrics are selected to compare the algorithms of the experimental group (PRA) and the control group.

(1) Sub-interval weight difference ΔO

The sub-interval weight difference ΔO is used to measure the difference in odor concentration weight generated by each algorithm within the same sub-interval, representing the algorithm's ability to control the travel cost within the sub-interval. The higher the odor concentration value is, the stronger the algorithm's ability to control the travel cost will be, and the lower the cost incurred by tourists moving within the sub-interval will also be. The sub-interval weight difference ΔO is defined as the difference between the odor concentration produced by the experimental group and the odor concentration produced by the control group within the same sub-interval. A positive difference indicates that the experimental group has a better ability to control the travel cost than the control group, while a negative difference indicates that the experimental group has a lower ability to control the travel cost than the control group.

(2) Route weight difference ΔO_{to}

The route weight difference ΔO_{to} is used to measure the difference in odor concentration weight generated by each algorithm for the entire route, representing the algorithm's ability to control the travel cost of the entire route. The higher the odor concentration value is, the stronger the algorithm's ability to control the travel cost will be, and the lower the cost incurred by tourists moving within the route will also be. The route weight difference ΔO_{to} is defined as the difference between the odor concentration generated by the experimental group and the odor concentration generated by the control group in the same route. A positive difference indicates that the experimental group has a better overall ability to control the travel cost than the control group, while a negative difference indicates that the experimental group has a lower overall ability to control the travel cost than the control group.

(3) Sub-interval mileage difference ΔS

Sub-interval mileage difference ΔS is directly used to measure the difference in the travel mileage generated by each algorithm within the same sub-interval. It is defined as the difference between the mileage generated by the control group and the mileage generated by the experimental group within the same sub-interval. A positive difference indicates that the travel cost generated by the control group is higher than that of the experimental group, while a negative difference indicates that the travel cost generated by the control group is lower than that of the experimental group.

(4) Route mileage difference ΔS_{to}

Route mileage difference ΔS_{to} is directly used to measure the difference in travel mileage generated by each algorithm for the same route. It is defined as the difference between the mileage generated by the control group and the mileage generated by the experimental group on the same route. A positive difference indicates that the travel cost generated by the control group is higher than that of the experimental group, while a

negative difference indicates that the travel cost generated by the control group is lower than that of the experimental group.

(5) Cost optimization ratio model Δc

The cost optimization ratio is used to represent the rate of cost reduction of the improved algorithm compared to the control group algorithm. In the comparative experiment, the cost optimization ratio Δc is used to measure the rate at which the experimental group algorithm reduces the route travel cost compared to the control group algorithm. By calculating the cost optimization ratio, the optimization degree of the experimental group algorithm can be intuitively obtained. The higher the cost optimization ratio is, the higher the cost reduction rate of the experimental group algorithm compared to the control group algorithm on a certain travel route. Formula (17) is the constructed cost optimization ratio model Δc, in which $S_{\exp}$ is the total distance of ICV route output by the experimental group and S_{con} is the total distance of ICV route output by the control group.

$$\Delta c = \frac{\left| S_{\exp} - S_{con} \right|}{S_{con}} \times 100\% \tag{17}$$

(6) Algorithm time complexity $O(n)$

The algorithm time complexity is determined by the algorithm design process and is used to measure the speed of the algorithm execution. The higher the time complexity is, the longer time the algorithm will run, and the lower the optimization degree of the algorithm will be; the lower the time complexity is, the shorter time the algorithm will run, and the higher the algorithm optimization degree will be. The comparative experiment uses time complexity to measure the running speed of the experimental group algorithm and the control group algorithms.

4.2.2. Data Collection

According to the experiment process and method, we collect the following experimental data.

(1) POIs within Chengdu city. POIs are classified according to their natural attributes and the results are shown in Table 1. The selection of POIs within the city meets the following conditions:

① POIs have feature attributes, including natural attributes. They must have four feature attributes: "travel cost", "travel time", "POI level" and "POI popularity", and must belong to one of the natural attributes of "park green land", "cultural and historical commemoration", "leisure shopping center", and "amusement and theme park".

② POIs are distributed within the urban area of Chengdu and are connected by various levels of urban roads, with strong spatial accessibility. POIs can be reached through local public transportation without the need for cross-city transportation.

③ POIs have definite spatial attributes, including longitude, latitude, and spatial distance, etc.

④ It is easy to obtain the POI information and data on the commonly used tourism official websites, including the natural attributes, feature attributes, and spatial attributes, etc.

(2) Representative ICV transfer stations. $IS_{(1)}$: Chadianzi Bus Station; $IS_{(2)}$: Tianfu Square; $IS_{(3)}$: Chengdu East Railway Station; $IS_{(4)}$: Chengdu Railway Station; $IS_{(5)}$: Chengdu South Railway Station. The five representative ICV transfer stations selected for the experiment are all the transportation hubs with the highest passenger flow, the longest operating hours, and located at the important control nodes in Chengdu city. They are distributed in the western, central, eastern, northern, and southern parts of Chengdu city, and are the most representative transportation hubs with the most significant geographical locations. Therefore, the five ICV transfer stations selected for the experiment can cover all the representative POIs, urban roads, and all the urban nodes within the experimental range, and their spatial locations are relatively

average to all the POIs. The longitude and latitude coordinates of the ICV transfer stations have typical spatial attributes, which can be used to quickly calculate the spatial accessibility with POIs and generate the spatial clusters.

Table 1. POI natural attribute classification.

Natural Attribute $G_{N(i)}$	POIs $P_{(i)}$ within the Research Range
Park and green land $G_{N(1)}$	$P_{(1)}$: People's Park; $P_{(9)}$: Tazishan Park; $P_{(11)}$: East Lake Park; $P_{(16)}$: Wangjianglou Park.
Cultural and historical commemoration $G_{N(2)}$	$P_{(2)}$: Sichuan Museum; $P_{(3)}$: Kuanzhai Alley; $P_{(6)}$: Du Fu Thatched Cottage; $P_{(7)}$: Eastern Suburb Memory; $P_{(8)}$: Wuhou Temple; $P_{(13)}$: Wenshu Temple; $P_{(14)}$: Jinsha Site.
Leisure shopping center $G_{N(3)}$	$P_{(4)}$: Chunxi Road; $P_{(10)}$: Jinniu Wanda; $P_{(12)}$: Raffles.
Amusement and theme park $G_{N(4)}$	$P_{(5)}$: Happy Valley; $P_{(15)}$: Guose Tianxiang Park.

(3) The feature attribute requirements for tourists that are input into the ICV decision-making system are shown in Table 2. Simultaneously, the feature attributes and spatial attributes of POIs are collected. Randomly select one tourist for the experiment and input his needs into the ICV decision-making system. To meet the matching algorithm between the tourist interests and POI feature attributes in POI recommendation, the demands that the tourist inputs into the ICV decision-making system should meet the following conditions:

① Travel cost x_1: $0 \leq x_1 \leq 250$, $x_1 \in \mathbf{R}$;
② Travel time x_2: $0 < x_2 \leq 5$, $x_2 \in \mathbf{R}$;
③ POI level x_3: $0 < x_3 \leq 5$, $x_3 \in \mathbf{N}$;
④ POI heat x_4: $0 < x_4 < 1$, $x_4 \in \mathbf{R}$.

Table 2. The input feature attribute requirements for the ICV decision-making system by the tourist.

Feature Attribute $f_{P(i)}$	Travel Cost x_1 (¥ Yuan)	Travel Time x_2 (Hour)	POI A-Class x_3 (A-LEVEL)	POI Popularity x_4
Tourist interest $f_{T(i)}$	$x_1 = 50$	$x_2 = 2$	$x_3 = 4$	$x_4 = 0.92$
Disturbance factor $\delta_{(i)}$	0.01	0.1	0.1	0.1

(4) Collect all road nodes between recommended POIs, and road nodes between POIs and ICV transfer stations. Collect road distances between adjacent road nodes. The process of collecting road nodes is as follows: ① Collect and determine all the ICV moving sub-intervals, and determine the starting and ending points of each sub-interval; ② Determine two control nodes for the ICV moving sub-interval, with each control node being an ICV transfer station or a POI; ③ Obtain all the connected roads between two control nodes in the city map, which can directly or indirectly connect the two control points; ④ Search for the road intersections from the starting control point to the ending control point. Encode each intersection when it is searched, and store it in the sub-interval node database; ⑤ Repeat the same searching for all sub-intervals; ⑥ Search for the distance between adjacent nodes in the city map and store it in the sub-interval node distance database.

4.3. Results and Analysis on POI Spatial Decision Forest and Topological Forest

4.3.1. Results on POI Feature Attribute Recommendation Degree and Spatial Decision Forest

We use the natural attribute classifications of POIs shown in Table 1 and the tourist requirements shown in Table 2, combined with the quantitative feature attributes of POIs,

and calculate the POI feature attribute recommendation degrees $\zeta(\mathbf{f}_{T(i)}, \mathbf{f}_{P(i)})$. The results are shown in Table 3.

Table 3. The output POI feature attribute recommendation degrees $\zeta(\mathbf{f}_{T(i)}, \mathbf{f}_{P(i)})$.

POI	$P_{(1)}$	$P_{(2)}$	$P_{(3)}$	$P_{(4)}$	$P_{(5)}$	$P_{(6)}$	$P_{(7)}$	$P_{(8)}$
$\zeta(\mathbf{f}_{T(i)}, \mathbf{f}_{P(i)})$	0.6317	0.6317	0.6500	0.6283	0.3557	0.9091	0.6667	0.9091
POI	$P_{(9)}$	$P_{(10)}$	$P_{(11)}$	$P_{(12)}$	$P_{(13)}$	$P_{(14)}$	$P_{(15)}$	$P_{(16)}$
$\zeta(\mathbf{f}_{T(i)}, \mathbf{f}_{P(i)})$	0.6317	0.6283	0.6317	0.6283	0.6623	0.8333	0.5481	0.6317

According to the constructed spatial decision tree algorithm, the experiment outputs the spatial decision tree $\mathbf{t}_{ree \cdot G_{N(i)}}$ corresponding to each natural attribute classification $G_{N(i)}$ and the spatial decision forest $\mathbf{f}_{orest \cdot G_{N(i)}}$ composed of decision trees, as shown in Figure 11. The values in the figure represent the feature attribute recommendation degree $\zeta(\mathbf{f}_{T(i)}, \mathbf{f}_{P(i)})$ of each POI. Figure 11(1) represents the decision tree $\mathbf{t}_{ree \cdot G_{N(1)}}$ of the natural attribute classification $G_{N(1)}$; Figure 11(2) represents the decision tree $\mathbf{t}_{ree \cdot G_{N(2)}}$ of the natural attribute classification $G_{N(2)}$; Figure 11(3) represents the decision tree $\mathbf{t}_{ree \cdot G_{N(3)}}$ of the natural attribute classification $G_{N(3)}$; and Figure 11(4) represents the decision tree $\mathbf{t}_{ree \cdot G_{N(4)}}$ of the natural attribute classification $G_{N(4)}$; the output spatial decision trees form a total spatial decision forest.

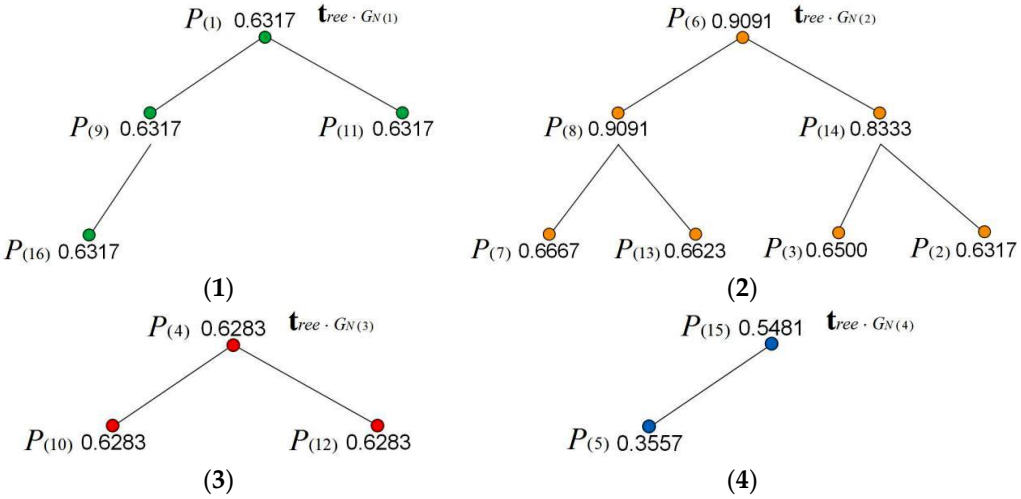

Figure 11. The spatial decision tree corresponding to each natural attribute classification and the spatial decision forest composed of decision trees. (**1**) represents the natural classification "park and green land"; (**2**) represents the natural classification "Cultural and historical commemoration"; (**3**) represents the natural attribute classification "Leisure shopping center"; (**4**) represents the natural attribute classification "Amusement and theme park".

4.3.2. Results on POI Spatial Topological Forest

The spatial accessibility $S_{A(IS_{(i)}, P_{(i)})}$ of POIs is calculated based on the geographical coordinates of each ICV transfer station $IS_{(i)}$. The results are shown in Table 4, and Table 5 shows the output topological matrix $\mathbf{S}_{A(i,j)}{}^{*}$ with each ICV transfer station as the seed point, in which $C_{(i)}$ is the cluster the POI belongs to. Based on the results in Tables 4 and 5 and the recommendation degrees in Table 3, as well as the spatial decision forest in Figure 11, the algorithm outputs the topological forest $\mathbf{f}_{orest \cdot G_{N(i)}}{}^{*}$ that integrates spatial accessibility $S_{A(IS_{(i)}, P_{(i)})}$, in which each decision tree $\mathbf{t}_{ree \cdot G_{N(i)}}$ still represents one natural classification $G_{N(i)}$. Figure 12 shows the formed topological forest labeled by the spatial accessibility.

Table 4. Calculation results on POI spatial accessibility $S_{A(IS_{(i)},P_{(i)})}$.

POI	$IS_{(1)}$	$IS_{(2)}$	$IS_{(3)}$	$IS_{(4)}$	$IS_{(5)}$	POI	$IS_{(1)}$	$IS_{(2)}$	$IS_{(3)}$	$IS_{(4)}$	$IS_{(5)}$
$P_{(1)}$	0.1493	1.1765	0.1124	0.2273	0.1639	$P_{(9)}$	0.0763	0.1639	0.5000	0.1235	0.1587
$P_{(2)}$	0.1818	0.3448	0.0926	0.1852	0.1408	$P_{(10)}$	0.1587	0.2778	0.1087	1.1905	0.1064
$P_{(3)}$	0.1639	0.7692	0.1053	0.2326	0.1493	$P_{(11)}$	0.0826	0.2083	0.1961	0.1190	0.3704
$P_{(4)}$	0.1220	0.7143	0.1471	0.2381	0.1639	$P_{(12)}$	0.1020	0.3333	0.1389	0.1370	0.3333
$P_{(5)}$	0.4348	0.1333	0.0694	0.2128	0.0752	$P_{(13)}$	0.1493	0.4762	0.1205	0.4348	0.1282
$P_{(6)}$	0.1818	0.2857	0.0885	0.1695	0.1408	$P_{(14)}$	0.3448	0.1786	0.0730	0.1613	0.0990
$P_{(7)}$	0.0877	0.1587	0.2083	0.1786	0.1099	$P_{(15)}$	0.0543	0.0413	0.0309	0.0415	0.0368
$P_{(8)}$	0.1299	0.4545	0.1087	0.1613	0.2041	$P_{(16)}$	0.0870	0.2381	0.2041	0.1266	0.2941

Table 5. The output topological matrix $\mathbf{S}_{A(i,j)}{}^{*}$ and spatial cluster $C_{(i)}$ by POI spatial accessibility.

Cluster	POIs Belonging to the Cluster
$C_{(1)} \sim IS_{(1)}$	$P_{(5)} - 0.4348$, $P_{(14)} - 0.3448$, $P_{(15)} - 0.0543$
$C_{(2)} \sim IS_{(2)}$	$P_{(1)} - 1.1765$, $P_{(2)} - 0.3448$, $P_{(3)} - 0.7692$, $P_{(4)} - 0.7143$, $P_{(6)} - 0.2857$, $P_{(8)} - 0.4545$, $P_{(13)} - 0.4762$
$C_{(3)} \sim IS_{(3)}$	$P_{(7)} - 0.2083$, $P_{(9)} - 0.5000$
$C_{(4)} \sim IS_{(4)}$	$P_{(10)} - 1.1905$
$C_{(5)} \sim IS_{(5)}$	$P_{(11)} - 0.3704$, $P_{(12)} - 0.3333$, $P_{(16)} - 0.2941$

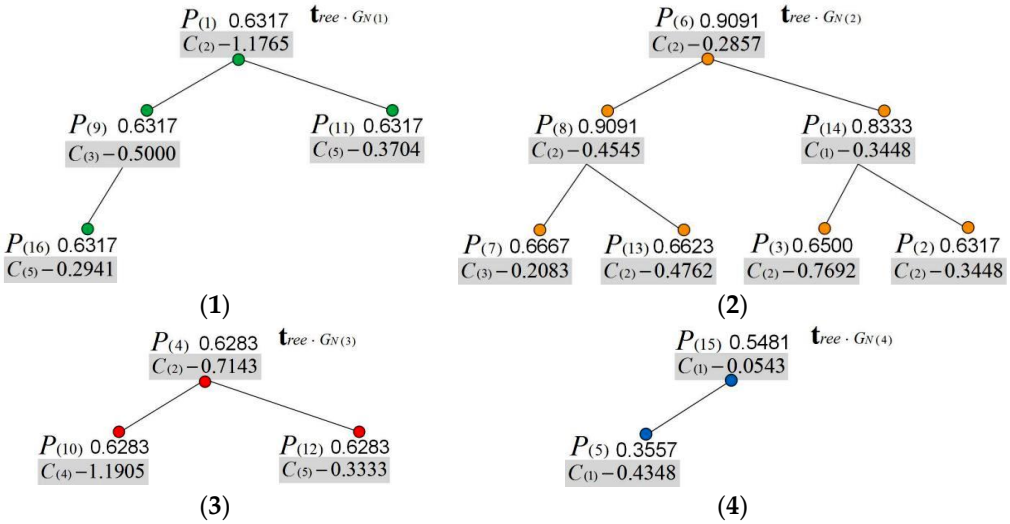

Figure 12. The formed topological forest labeled by spatial accessibility. (**1**) represents the natural classification "park and green land"; (**2**) represents the natural classification "Cultural and historical commemoration"; (**3**) represents the natural attribute classification "Leisure shopping center"; (**4**) represents the natural attribute classification "Amusement and theme park".

4.3.3. Results Analysis on the POI Feature Attribute Recommendation Degree, Spatial Decision Forest and POI Spatial Topological Forest

Analyzing the POI feature attribute recommendation degree results in Table 3, when the tourist inputs the feature attribute requirements to the ICV decision-making system, the system outputs the POI feature attribute recommendation results. Due to the different feature attributes of POIs, the calculated recommendation degrees are different. Under the interest requirement condition of the sample tourist, $P_{(6)}$: Du Fu Thatched Cottage, and $P_{(8)}$: Wuhou Temple have the highest recommendation degree, both of which are 0.9091. Next is $P_{(14)}$: Jinsha Site, with a recommendation degree of 0.8333. The POI recommendation degrees of the majority samples are distributed in the range of 0.6–0.7, with an average value of 0.6611, indicating that the POIs have strong overall ability to meet the tourist's interests.

The recommendation degree variance is 0.0178, and the standard deviation is 0.1333, indicating that the ability of each sample POI to meet the tourist's interests is relatively balanced, with small dispersion. That is to say, all POIs can meet the tourist's interests, and there is no apparent difference in function and capacity. The recommendation degree mode is 0.6317, indicating that the POIs with recommendation degree of 0.6317 appear most frequently and are relatively concentrated. These POIs have similar ability to meet the tourist's interests. By analyzing the distribution, average value, variance, standard deviation, and mode of recommendation degrees, it can be concluded that the proposed feature attribute recommendation algorithm has good stability and can objectively express the relationship between tourists' interests and the POI feature attributes. Analyzing the feature attribute decision forest output in Figure 8, each natural classification represents a decision tree, and the POIs within the same tree have the same natural attributes. The root node of the tree represents the POI with the highest recommendation degree in the natural classification. The recommendation degrees of the child nodes of the tree are smaller. The decision forest of the ICV system provides the tourists with a visual recommendation schedule, allowing them to directly select the POIs with the highest recommendation degrees among various natural classifications.

The POI spatial accessibility results in Table 4 show that each POI has different spatial accessibility for different ICV transfer stations, showing a fluctuating trend. The higher the spatial accessibility is, the higher the spatial closeness between the POI and the ICV transfer station will be, and the higher probability of belonging to the cluster where the ICV transfer station is located will also be. Among all the ICV transfer stations, the ICV transfer station with the highest spatial accessibility is the transfer station with the highest spatial closeness with the POI, and the POI belongs to its spatial cluster. Table 5 shows the ICV transfer station clusters where each POI is located, which are output by the constructed spatial clustering algorithm. The values after POIs represent their spatial accessibility to the transfer stations in the cluster they are located in. The results in Tables 4 and 5 demonstrate that the proposed spatial attribute clustering algorithm has good clustering performance, which can measure the spatial relationship between the POIs and the ICV transfer stations and realize the spatial clustering.

4.4. Results and Analysis on Recommendation Degree, Recommendation Degree Decision Forest and Recommended POI

4.4.1. Results on Recommendation Degree, Recommendation Degree Decision Forest and Recommended POIs

The experiment sets that the sample tourist has different requirements for the POI feature attributes and spatial attributes. The interest weight for the feature attribute factor is 0.6, and the interest weight for the spatial attribute is 0.4. The tourist expects to visit two POIs in the natural classification of $G_{N(1)}$ "park and green land", one POI in $G_{N(2)}$ "cultural and historical commemoration", and one POI in $G_{N(3)}$ "leisure shopping center". According to the results in Tables 3–5, the POI recommendation degrees $\zeta_{P_{(i)}}$ of the ICV navigation routes are calculated, and the results are shown in Table 6. According to the results in Table 6, the experiment outputs the decision trees $\mathbf{t}_{ree \cdot G_{N(i)}}$ and the decision forest $\mathbf{f}_{orest \cdot G_{N(i)}}{}^{*}$ containing the clusters $C_{(i)}$ and the recommendation degrees $\zeta_{P_{(i)}}$, as shown in Figure 13, in which each decision tree $\mathbf{t}_{ree \cdot G_{N(i)}}$ still represents one natural classification. According to the results in Table 6 and Figure 13, the POIs recommended by the ICV decision-making system for the tourists are the POIs at the root nodes of the decision trees, including $P_{(1)}$: People's Park, $P_{(9)}$: Tazishan Park, $P_{(8)}$: Wuhou Temple, and $P_{(10)}$: Jinniu Wanda.

Table 6. The results on POI recommendation degree $\zeta_{P_{(i)}}$ for ICV navigation route.

POI	$P_{(1)}$	$P_{(2)}$	$P_{(3)}$	$P_{(4)}$	$P_{(5)}$	$P_{(6)}$	$P_{(7)}$	$P_{(8)}$
$\zeta_{P_{(i)}}$	0.8496	0.5169	0.6977	0.6627	0.3874	0.6597	0.4833	0.7273
POI	$P_{(9)}$	$P_{(10)}$	$P_{(11)}$	$P_{(12)}$	$P_{(13)}$	$P_{(14)}$	$P_{(15)}$	$P_{(16)}$
$\zeta_{P_{(i)}}$	0.5790	0.8532	0.5272	0.5103	0.5879	0.6379	0.3506	0.4967

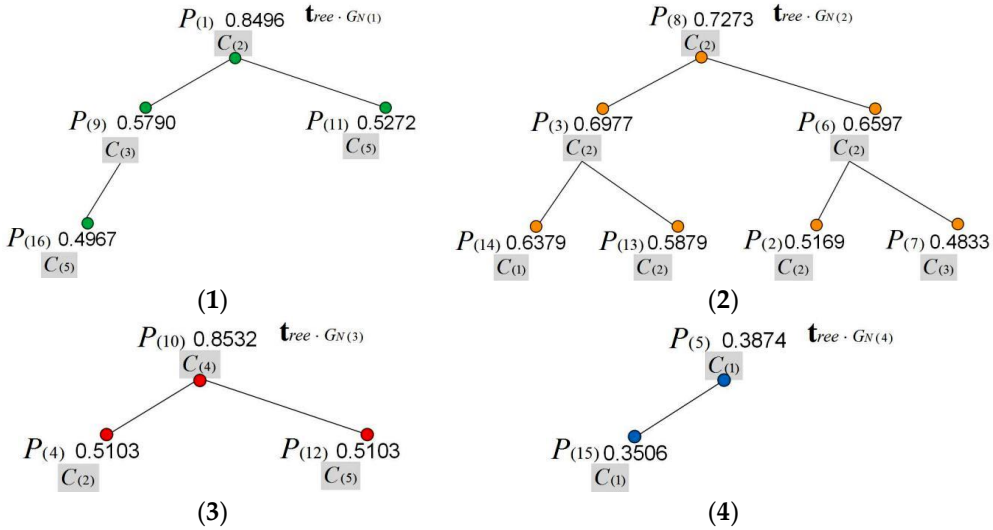

Figure 13. Decision tree and decision forest including cluster and recommendation degree. (**1**) represents the natural classification "Park and green land"; (**2**) represents the natural classification "Cultural and historical commemoration"; (**3**) represents the natural attribute classification "Leisure shopping center"; (**4**) represents the natural attribute classification "Amusement and theme park".

4.4.2. Results Analysis on the Recommendation Degree, Recommendation Degree Decision Forest and Recommended POI

Analyzing the POI recommendation results for the ICV navigation route in Table 6, when a tourist inputs the feature attribute weight and the spatial attribute weight to the ICV decision-making system, the system outputs the POI recommendation results. Due to the different feature attributes and spatial attributes of POI, the calculated recommendation degrees are discrepant. Under the interest requirement conditions of the sample tourist, $P_{(10)}$: Jinniu Wanda has the highest recommendation degree, which is 0.8532. The next is $P_{(1)}$: People's Park, with a recommendation degree of 0.8496. The recommendation degrees of the majority POI samples are distributed in the range of 0.5 to 0.7, with an average recommendation degree of 0.5955, indicating that these POIs have strong overall ability to meet the tourist's interests. The recommendation degree variance is 0.0209, and the standard deviation is 0.1445, indicating that the ability of each sample POI to meet the tourist's interests is relatively balanced, with small dispersion; that is, all POIs can meet the feature attribute and spatial attribute requirements proposed by the tourist, and there is no apparent difference in function and capacity. By analyzing the distribution, average value, variance, and standard deviation of recommendation degrees, it can be concluded that the proposed POI recommendation algorithm for the ICV navigation route has good stability and can objectively express the relationship between the tourists' interests and the POI attributes, outputting the optimal POIs on the ICV navigation route. Analyzing the decision forest in Figure 13, each natural classification represents a decision tree, and the POIs within the same tree have the same natural attributes. The root node of the tree represents the POI in the natural classification with the highest recommendation degree of the ICV navigation route. The recommendation degrees of the child nodes are smaller. When the tourists determine the feature attribute weight and the spatial attribute weight,

the recommendation degree of each POI varies significantly from Figure 11, indicating that the POIs on the ICV navigation route are the optimal POIs that both meet the feature attributes and the spatial attributes, as well as the weight requirements. The decision forest of the ICV system provides the tourists with a visual recommendation schedule, allowing them to directly select the POIs with the highest recommendation among various natural classifications from the decision tree.

4.5. Results and Analysis on ICV Navigation Route

4.5.1. Results on ICV Navigation Route

According to the results, the recommended optimal POIs are $P_{(1)}$: People's Park, $P_{(8)}$: Wuhou Temple, $P_{(9)}$: Tazishan Park, and $P_{(10)}$: Jinniu Wanda, as well as the tourist departure ICV transfer station $IS_{(1)}$: Chadianzi Bus Station, and the destination ICV transfer station $IS_{(3)}$: Chengdu East Railway Station. In the experiment, the proposed improved fruit fly optimization algorithm is used to output the fruit fly odor concentration $O(f_{R_{sub(i,j)}})$ in each ICV navigation route sub-interval $R_{sub(i)}$, and output the iterative value of the fruit fly odor concentration $O(f_{R_{sub(i,j)}})_{to}$ in the whole navigation route. The results are shown in Table 7; "$P_{a,b,c,d}$" represents the ICV navigation route "$IS_{(1)} - P_{(a)} - P_{(b)} - P_{(c)} - P_{(d)} - IS_{(3)}$".

Table 7. The odor concentration $O(f_{R_{sub(i,j)}})$ in each sub-interval and the iterative value of odor concentration $O(f_{R_{sub(i,j)}})_{to}$ in the ICV navigation route.

Route	$O(f_{R_{sub(i,j)}})$					$O(f_{R_{sub(i,j)}})_{to}$	Route	$O(f_{R_{sub(i,j)}})$					$O(f_{R_{sub(i,j)}})_{to}$
	R1	**R2**	**R3**	**R4**	**R5**			**R1**	**R2**	**R3**	**R4**	**R5**	
$P_{1,8,9,10}$	0.1235	0.3704	0.1163	0.0885	0.0917	0.7903	$P_{9,1,8,10}$	0.0541	0.1235	0.3704	0.1639	0.0917	0.8036
$P_{1,8,10,9}$	0.1235	0.3704	0.1639	0.0885	0.3226	1.0688	$P_{9,1,10,8}$	0.0541	0.1235	0.2041	0.1639	0.0901	0.6356
$P_{1,9,8,10}$	0.1235	0.1235	0.1163	0.1639	0.0917	0.6189	$P_{9,8,1,10}$	0.0541	0.1163	0.3704	0.2041	0.0917	0.8365
$P_{1,9,10,8}$	0.1235	0.1235	0.0885	0.1639	0.0901	0.5894	$P_{9,8,10,1}$	0.0541	0.1163	0.1639	0.2041	0.1075	0.6459
$P_{1,10,8,9}$	0.1235	0.2041	0.1639	0.1163	0.3226	0.9303	$P_{9,10,1,8}$	0.0541	0.0885	0.2041	0.3704	0.0901	0.8071
$P_{1,10,9,8}$	0.1235	0.2041	0.0885	0.1163	0.0901	0.6224	$P_{9,10,8,1}$	0.0541	0.0885	0.1639	0.3704	0.1075	0.7844
$P_{8,1,9,10}$	0.1031	0.3704	0.1235	0.0885	0.0917	0.7772	$P_{10,1,8,9}$	0.1099	0.2041	0.3704	0.1163	0.3226	1.1232
$P_{8,1,10,9}$	0.1031	0.3704	0.2041	0.0885	0.3226	1.0886	$P_{10,1,9,8}$	0.1099	0.2041	0.1235	0.1163	0.0901	0.6438
$P_{8,9,1,10}$	0.1031	0.1163	0.1235	0.2041	0.0917	0.6387	$P_{10,8,1,9}$	0.1099	0.1639	0.3704	0.1235	0.3226	1.0902
$P_{8,9,10,1}$	0.1031	0.1163	0.0885	0.2041	0.1075	0.6195	$P_{10,8,9,1}$	0.1099	0.1639	0.1163	0.1235	0.1075	0.6211
$P_{8,10,1,9}$	0.1031	0.1639	0.2041	0.1235	0.3226	0.9171	$P_{10,9,1,8}$	0.1099	0.0885	0.1235	0.3704	0.0901	0.7823
$P_{8,10,9,1}$	0.1031	0.1639	0.0885	0.1235	0.1075	0.5865	$P_{10,9,8,1}$	0.1099	0.0885	0.1163	0.3704	0.1075	0.7926

Based on the map of Chengdu, as well as the geographical locations of the ICV transfer stations $IS_{(i)}$ and the recommended POIs, the experiment extracts the coordinates of the starting station $IS_{(1)}$, terminal station $IS_{(3)}$, and POIs $P_{(1)}$, $P_{(8)}$, $P_{(9)}$, and $P_{(10)}$, and outputs the trend curves of the three optimal ICV navigation routes. The relationship between each POI and the ICV transfer station $IS_{(i)}$ in its cluster is labeled. Figure 14(1,2) show the spatial distributions between the ICV transfer stations and the recommended POIs; Figure 14(3) shows the sub-interval network composed of the ICV transfer stations and the recommended POIs; Figure 14(4) shows the optimal ICV navigation route, while Figure 14(5,6) show the two suboptimal navigation routes.

4.5.2. Results Analysis on ICV Navigation Route

Analyzing the results in Table 7, the proposed improved fruit fly optimization algorithm can find out the optimal fruit fly individual and corresponding odor concentration function value in each sub-interval, making the ICV path in the sub-interval corresponding to the optimal fruit fly individual be the shortest, and ultimately minimizing the ICV travel cost. By outputting the optimal fruit fly individuals within the multiple sub-intervals of the ICV navigation route, iteratively output the overall odor concentration value of each feasible ICV navigation route. The overall odor concentration value of each ICV navigation

route reflects the quality and cost of the ICV route. From the data in Table 7, it can be seen that in this experiment, the starting point $IS_{(1)}$, terminal point $IS_{(3)}$, as well as the POIs $P_{(1)}$, $P_{(8)}$, $P_{(9)}$, and $P_{(10)}$, all come from the ICV navigation route. Each ICV navigation route is composed of five sub-intervals. The odor concentration function values of each sub-interval output by the improved fruit fly optimization algorithm are different, showing a fluctuating trend. The total odor concentration of the ICV navigation route generated by this iteration is also different, showing a fluctuating trend. The results show that the three ICV navigation routes with the highest odor concentration iteration values are:

① Optimal ICV navigation route ($P_{10,1,8,9}$):
$IS_{(1)} - P_{(10)} - P_{(1)} - P_{(8)} - P_{(9)} - IS_{(3)}$, with the odor concentration: 1.1232;
② Suboptimal ICV navigation route 1 ($P_{10,8,1,9}$):
$IS_{(1)} - P_{(10)} - P_{(8)} - P_{(1)} - P_{(9)} - IS_{(3)}$, with the odor concentration: 1.0902;
③ Suboptimal ICV navigation route 2 ($P_{8,1,10,9}$):
$IS_{(1)} - P_{(8)} - P_{(1)} - P_{(10)} - P_{(9)} - IS_{(3)}$, with the odor concentration: 1.0886;

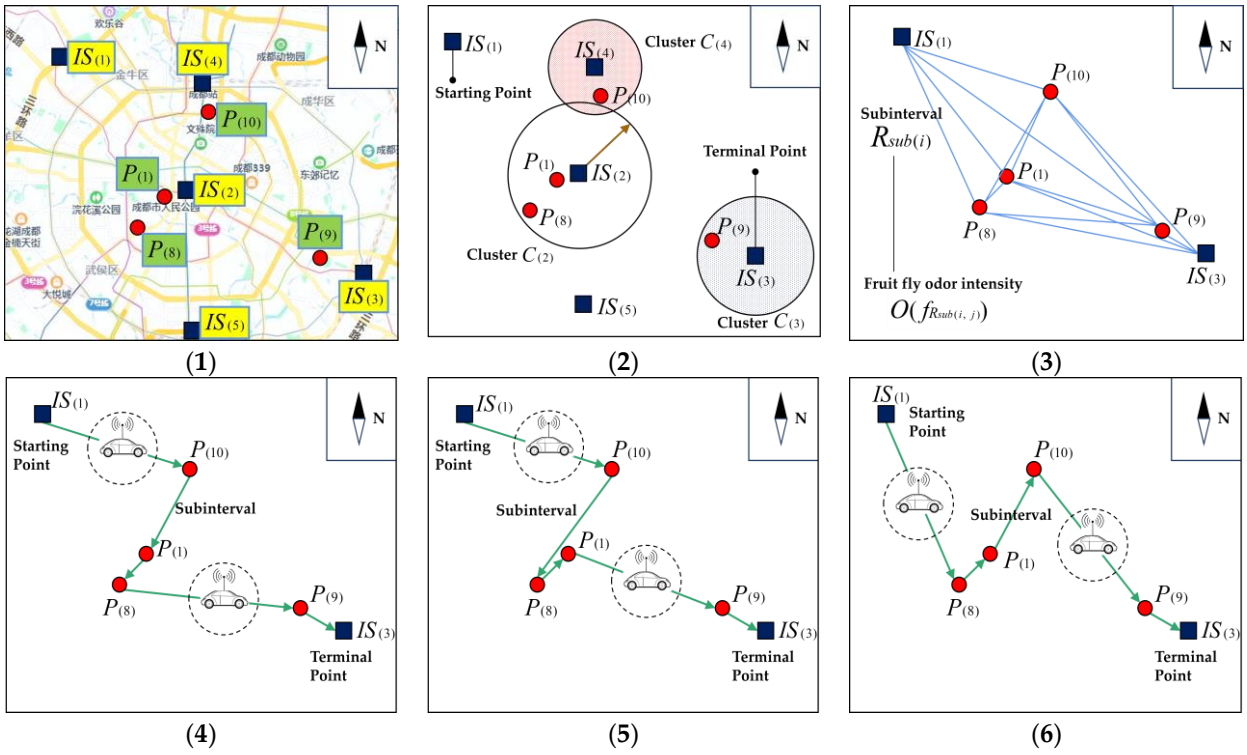

Figure 14. The spatial relationship between ICV and POI and three optimal ICV navigation routes. (**1**,**2**) show the spatial distributions between ICV transfer stations and recommended POIs; (**3**) shows the sub-interval network composed of ICV transfer stations and recommended POIs; (**4**) shows the optimal ICV navigation route, while (**5**,**6**) show two suboptimal navigation routes.

From the results, it can be concluded that the travel cost incurred by the tourist traveling along the ICV navigation route "$P_{10,1,8,9}$" is the lowest, followed by the navigation routes "$P_{10,8,1,9}$" and "$P_{8,1,10,9}$". The experimental results show that the proposed improved fruit fly optimization algorithm can find out the fruit fly individual with the lowest travel cost in the sub-interval of the route, and ultimately output the ICV navigation route with the lowest travel cost.

Analyzing the visualization results in Figure 14, it can be concluded from Figure 14(1,2) that the recommended POIs belong to the different ICV transfer station spatial clusters, which makes the POIs have the feature of approaching the ICV navigation route with the lowest cost. The constructed fruit fly optimization algorithm is limited to the range of the optimal spatial distribution, as shown in Figure 14(3); it can thereby further reduce

the spatial cost of the ICV navigation routes, output the global optimal ICV navigation route, and effectively reduce the travel cost of ICV. Figure 14(4–6) show the optimal ICV navigation route and two suboptimal routes respectively. From the analysis of the optimal route shape and trend, it can be concluded that the route with the lowest ICV travel cost have the following characteristics:

① Fluctuate and approach from the starting point to the terminal point along the virtual connecting line between the starting point and the terminal point;

② There is no path crossing in sub-interval;

③ There is no closed-loop structure, namely, the sub-interval does not form any closed path;

④ There is no return route.

4.6. Results and Analysis on the Comparative Experiment

4.6.1. Method and Results of the Comparative Experiment

In the ICV navigation route planning, the ICV decision-making system generally uses its own electronic map for route planning. The commonly used ICV route maps include the Gaode Map and the Baidu Map, etc., which use embedded algorithms to search for the path of ICVs from the starting point to the destination. In the comparative experiment, we select the Gaode Map (GDA) and the Baidu Map (BDA), which are most commonly used in ICV navigation route planning, as the control group. The improved fruit fly optimization algorithm (IFOA-PRA) constructed in this paper is set as the experimental group. Under the same experimental conditions, The GDA and BDA, respectively, search for the shortest distance in each sub-interval, calculate the sub-interval weight, and iteratively output the ICV route weight and the optimal three ICV routes. Compare the three optimal ICV routes between the experimental group and the control group, and then compare the ICV route-planning methods from the following aspects: sub-interval weight difference ΔO, route weight difference ΔO_{to}, sub-interval mileage difference ΔS, route mileage difference ΔS_{to}, and cost optimization ratio Δc.

Other commonly used route-searching algorithms include Dijkstra and Floyd–Warshall, etc. Set algorithms of the Dijkstra (DIJA) and the Floyd Warhill (FWA) as the control group, the proposed improved fruit fly optimization algorithm (IFOA-PRA) as the experimental group. Under the same experimental conditions, the DIJA and the FWA respectively search for the shortest distance in each sub-interval, calculate the sub-interval weight, and iteratively output the ICV route weight and the optimal three ICV routes. Compare the three optimal ICV routes between the experimental group and the control group, and then compare the ICV route-planning methods from the following aspects: sub-interval weight difference ΔO, route weight difference ΔO_{to}, sub-interval mileage difference ΔS, route mileage difference ΔS_{to}, cost optimization ratio Δc, and algorithm time complexity.

(1) The results shown in Table 8 are the comparison of the sub-interval weight $O(f_{R_{sub(i,j)}})$ and the route weight $O(f_{R_{sub(i,j)}})_{to}$ of the optimal ICV navigation route ICV-G1, and the suboptimal navigation routes ICV-G2 and ICV-G3 output by the three algorithms. The results shown in Table 9 are the comparison of the optimal and suboptimal ICV navigation routes in the sub-interval weight difference ΔO, route weight difference ΔO_{to}, and cost optimization ratio Δc, between the control group and the experimental group. Figure 15 shows the comparison of the sub-interval weight difference ΔO, route weight difference ΔO_{to}, and cost optimization ratio Δc, between the control group and the experimental group. Figure 15(1) represents the comparison between the GDA and the PRA. Figure 15(2) represents the comparison between the BDA and the PRA. Figure 15(3) represents the comparison between the DIJA and the PRA. Figure 15(4) represents the comparison between the FWA and the PRA. In each figure, the blue data columns represent the route $P_{10,1,8,9}$, the brown data columns represent the route $P_{10,8,1,9}$, and the green data columns represent the route $P_{8,1,10,9}$.

(2) The results shown in Table 10 are the comparison of sub-interval mileage S and total route mileage S_{to} of the optimal ICV guidance route ICV-G1, and the suboptimal

guidance routes ICV-G2 and ICV-G3 output by each method of the control group and the experimental group. The results shown in the Table 11 are the comparisons of the sub-interval mileage difference ΔS, total route mileage difference ΔS_{to}, and cost optimization rate Δc of the optimal and suboptimal ICV guidance routes output by each method, between the control group and the experimental group. Figure 16 shows the comparison of sub-interval mileage difference ΔS, route mileage difference ΔS_{to}, and cost optimization rate Δc between the control group algorithms and the experimental group algorithm. Figure 16(1) represents the comparison between the GDA and the PRA. Figure 16(2) represents the comparison between the BDA and the PRA. Figure 16(3) represents the comparison between the DIJA and the PRA. Figure 16(4) represents the comparison between the FWA and the PRA. In each figure, the blue data columns represent the route $P_{10,1,8,9}$, the brown data columns represent the route $P_{10,8,1,9}$, and the green data column represents the route $P_{8,1,10,9}$.

(3) Table 12 shows the time complexity comparisons between the route-searching algorithm (PRA), the DIJA, and the FWA. According to the constraints of the urban geographic space and the tourism scenarios, the number of the sub-interval nodes is usually within 10, and the number of the POIs visited by the tourists within a day does not exceed 10. Therefore, the value range of the algorithm nodes is set as $0 < n \leq 10, n \in \mathbf{N}$. Figure 17 shows the comparisons of the time complexity of the proposed algorithm (PRA), the DIJA, and the FWA under the different node numbers. Figure 17(1) shows the comparison curve of time complexity, and Figure 17(2) shows the comparison chart of the time complexity.

Table 8. The comparison of the sub-interval weight $O(f_{R_{sub(i,j)}})$ and route weight $O(f_{R_{sub(i,j)}})_{to}$ of the algorithms.

		Route	$O(f_{R_{sub(i,j)}})$					$O(f_{R_{sub(i,j)}})_{to}$
			R1	R2	R3	R4	R5	
PRA	ICV-G1	$P_{10,1,8,9}$	0.1099	0.2041	0.3704	0.1163	0.3226	1.1232
	ICV-G2	$P_{10,8,1,9}$	0.1099	0.1639	0.3704	0.1235	0.3226	1.0902
	ICV-G3	$P_{8,1,10,9}$	0.1031	0.3704	0.2041	0.0885	0.3226	1.0886
GDA	ICV-G1	$P_{10,1,8,9}$	0.1064	0.1887	0.2857	0.1111	0.2857	0.9776
	ICV-G2	$P_{10,8,1,9}$	0.1064	0.1471	0.2857	0.1205	0.2857	0.9454
	ICV-G3	$P_{8,1,10,9}$	0.0943	0.2857	0.1887	0.0806	0.2857	0.9351
BDA	ICV-G1	$P_{10,8,1,9}$	0.1031	0.1493	0.2564	0.1220	0.2564	0.8871
	ICV-G2	$P_{10,1,8,9}$	0.1031	0.1667	0.2564	0.1000	0.2564	0.8826
	ICV-G3	$P_{8,1,10,9}$	0.0870	0.2564	0.1667	0.0855	0.2564	0.8519
DIJA	ICV-G1	$P_{10,1,8,9}$	0.1031	0.1887	0.2857	0.1111	0.3226	0.9081
	ICV-G2	$P_{10,8,1,9}$	0.1031	0.1639	0.2857	0.1235	0.3226	0.8957
	ICV-G3	$P_{8,1,10,9}$	0.1031	0.2857	0.1887	0.0806	0.3226	0.8776
FWA	ICV-G1	$P_{10,1,8,9}$	0.1064	0.2041	0.3704	0.1163	0.3226	1.1197
	ICV-G2	$P_{10,8,1,9}$	0.1064	0.1639	0.3704	0.1220	0.3226	1.0852
	ICV-G3	$P_{8,1,10,9}$	0.1031	0.3704	0.2041	0.0806	0.3226	1.0808

Table 9. The comparison of the optimal and suboptimal ICV navigation routes in sub-interval weight difference ΔO route weight difference ΔO_{to} and cost optimization ratio Δc of the algorithms.

	Route	ΔO					ΔO_{to}	Δc
		R1	R2	R3	R4	R5		
PRA-GDA	$P_{10,1,8,9}$	0.0035	0.0154	0.0847	0.0052	0.0369	0.1456	7.49%
	$P_{10,8,1,9}$	0.0035	0.0168	0.0847	0.0030	0.0369	0.1448	7.62%
	$P_{8,1,10,9}$	0.0088	0.0847	0.0154	0.0079	0.0369	0.1535	10.20%

Table 9. *Cont.*

	Route	ΔO					ΔO_{to}	Δc
		R1	R2	R3	R4	R5		
PRA-BDA	$P_{10,1,8,9}$	0.0068	0.0374	0.1140	0.0163	0.0662	0.2406	15.22%
	$P_{10,8,1,9}$	0.0068	0.0146	0.1140	0.0015	0.0662	0.2031	10.19%
	$P_{8,1,10,9}$	0.0161	0.1140	0.0374	0.0030	0.0662	0.2367	14.32%
PRA-DIJA	$P_{10,1,8,9}$	0.0068	0.0154	0.0847	0.0052	0	0.2151	7.19%
	$P_{10,8,1,9}$	0.0068	0	0.0847	0	0	0.1945	4.59%
	$P_{8,1,10,9}$	0	0.0847	0.0154	0.0079	0	0.2110	6.76%
PRA-FWA	$P_{10,1,8,9}$	0.0035	0	0	0	0	0.0035	1.05%
	$P_{10,8,1,9}$	0.0035	0	0	0.0015	0	0.0050	1.36%
	$P_{8,1,10,9}$	0	0	0	0.0079	0	0.0078	3.35%

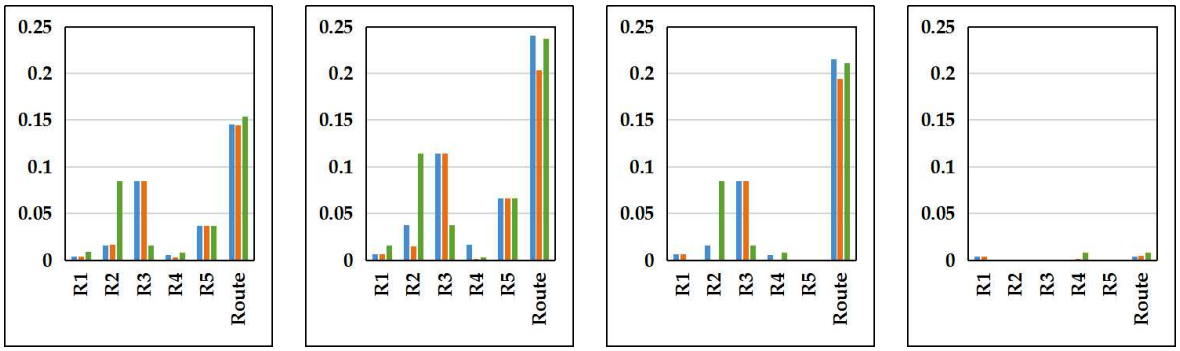

Figure 15. The comparison of sub-interval weight difference ΔO, route weight difference ΔO_{to}, and cost optimization ratio Δc between the control group algorithms and the experimental group algorithm. (**1**) represents the comparison between GDA and PRA, (**2**) represents the comparison between BDA and PRA, (**3**) represents the comparison between DIJA and PRA, and (**4**) represents the comparison between FWA and PRA. In each figure, the blue data columns represent route $P_{10,1,8,9}$, the brown data columns represent route $P_{10,8,1,9}$, and the green data columns represent route $P_{8,1,10,9}$.

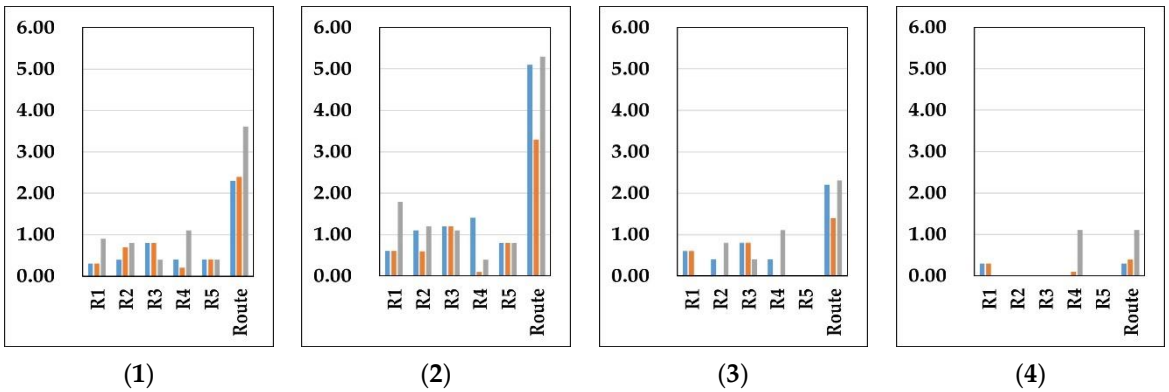

Figure 16. The comparison of sub-interval mileage difference ΔS, route mileage difference ΔS_{to}, and cost optimization rate Δc between the control group algorithms and the experimental group algorithm. (**1**) represents the comparison between GDA and PRA, (**2**) represents the comparison between BDA and PRA, (**3**) represents the comparison between DIJA and PRA, and (**4**) represents the comparison between FWA and PRA. In each figure, the blue data columns represent route $P_{10,1,8,9}$, the brown data columns represent route $P_{10,8,1,9}$, and the grey data column represents route $P_{8,1,10,9}$.

Table 10. The comparison on sub-interval mileage $S(f_{R_{sub(i,j)}})$ and route mileage $S(f_{R_{sub(i,j)}})_{to}$ between the control group algorithms and the experimental group algorithm.

		Route	$S(f_{R_{sub(i,j)}})$					$S(f_{R_{sub(i,j)}})_{to}$
			R1	R2	R3	R4	R5	
PRA	ICV-G1	$P_{10,1,8,9}$	9.0992	4.8996	2.6998	8.5985	3.0998	28.3968
	ICV-G2	$P_{10,8,1,9}$	9.0992	6.1013	2.6998	8.0972	3.0998	29.0972
	ICV-G3	$P_{8,1,10,9}$	9.6993	2.6998	4.8996	11.2994	3.0998	31.6979
GDA	ICV-G1	$P_{10,1,8,9}$	9.3985	5.2994	3.5002	9.0009	3.5002	30.6992
	ICV-G2	$P_{10,8,1,9}$	9.3985	6.7981	3.5002	8.2988	3.5002	31.4957
	ICV-G3	$P_{8,1,10,9}$	10.6045	3.5002	5.2994	12.4069	3.5002	35.3112
BDA	ICV-G1	$P_{10,8,1,9}$	9.6993	6.6979	3.9002	8.1967	3.9002	32.3943
	ICV-G2	$P_{10,1,8,9}$	9.6993	5.9988	3.9002	10.0000	3.9002	33.4984
	ICV-G3	$P_{8,1,10,9}$	11.4943	3.9002	5.9988	11.6959	3.9002	36.9893
DIJA	ICV-G1	$P_{10,1,8,9}$	9.6993	5.2994	3.5002	9.0009	3.0998	30.5996
	ICV-G2	$P_{10,8,1,9}$	9.6993	6.1013	3.5002	8.0972	3.0998	30.4978
	ICV-G3	$P_{8,1,10,9}$	9.6993	3.5002	5.2994	12.4069	3.0998	34.0057
FWA	ICV-G1	$P_{10,1,8,9}$	9.3985	4.8996	2.6998	8.5985	3.0998	28.6961
	ICV-G2	$P_{10,8,1,9}$	9.3985	6.1013	2.6998	8.1967	3.0998	29.4961
	ICV-G3	$P_{8,1,10,9}$	9.6993	2.6998	4.8996	12.4069	3.0998	32.8054

Table 11. The comparison on the sub-interval mileage difference ΔS, route mileage difference ΔS_{to}, and cost optimization rate Δc between the control group algorithms and the experimental group algorithm.

	Route	ΔS					ΔS_{to}	Δc
		R1	R2	R3	R4	R5		
GDA-PRA	$P_{10,1,8,9}$	0.2993	0.3999	0.8004	0.4024	0.4004	2.3024	7.49%
	$P_{10,8,1,9}$	0.2993	0.6968	0.8004	0.2016	0.4004	2.3985	7.62%
	$P_{8,1,10,9}$	0.9051	0.8004	0.3999	1.1075	0.4004	3.6133	10.20%
BDA-PRA	$P_{10,1,8,9}$	0.6001	1.0992	1.2004	1.4015	0.8003	5.1016	15.22%
	$P_{10,8,1,9}$	0.6001	0.5966	1.2004	0.0996	0.8003	3.2971	10.19%
	$P_{8,1,10,9}$	1.7949	1.2004	1.0992	0.3965	0.8003	5.2914	14.32%
DIJA-PRA	$P_{10,1,8,9}$	0.6001	0.3999	0.8004	0.4024	0.0000	2.2028	7.19%
	$P_{10,8,1,9}$	0.6001	0.0000	0.8004	0.0000	0.0000	1.4005	4.59%
	$P_{8,1,10,9}$	0.0000	0.8004	0.3999	1.1075	0.0000	2.3078	6.76%
FWA-PRA	$P_{10,1,8,9}$	0.2993	0.0000	0.0000	0.0000	0.0000	0.2993	1.05%
	$P_{10,8,1,9}$	0.2993	0.0000	0.0000	0.0996	0.0000	0.3989	1.36%
	$P_{8,1,10,9}$	0.0000	0.0000	0.0000	1.1075	0.0000	1.1075	3.38%

Table 12. The comparison of time complexity (TC) level between the control group algorithms and the experimental group algorithm (time unit: nanoseconds).

	TC	n=1	n=2	n=3	n=4	n=5	n=6	n=7	n=8	n=9	n=10
PRA	$O(n)$	1	2	3	4	5	6	7	8	9	10
DIJA	$O(n^2)$	1	4	9	16	25	36	49	64	81	100
FWA	$O(n^3)$	1	8	27	64	125	216	343	512	729	1000

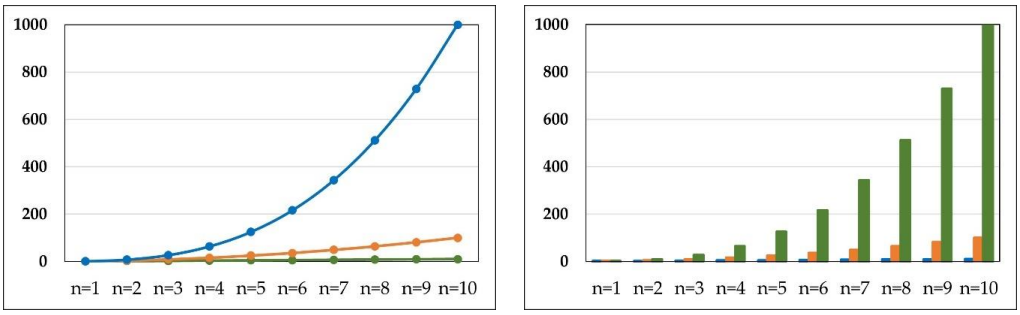

Figure 17. The comparison of the time complexity of the proposed algorithm (PRA), DIJA, and FWA under the different node numbers. (**1**) shows the comparison curve of time complexity, and (**2**) shows the comparison chart of the time complexity. In (**1**), the blue color represents the FWA, the yellow color represents the DIJA, the green color represents the PRA. In (**2**), the blue color represents the PRA, the yellow color represents the DIJA, the green color represents the FWA.

4.6.2. Analysis of the Comparative Experimental Results

Analyzing the comparative experimental results of Tables 8–11, the proposed improved fruit fly optimization algorithm (PRA) has significant advantages in outputting the travel cost and weight of ICV navigation routes. The odor weights of the three ICV navigation routes in each sub-interval are higher than that of the map route-planning methods GDA and BDA; that is, the travel cost of the PRA method outputting ICV navigation route is lower than that of the GDA and the BDA. This will finally lead to a higher overall odor weight and lower travel cost for the ICV navigation route. Compared with the commonly used route-searching algorithms Dijkstra and Floyd–Warshall, the PRA also has significant advantages in outputting the travel cost and route weight of the ICV navigation routes. The odor weight of the three ICV navigation routes in each sub-interval is higher or equivalent than that of the DIJA and the FWA, and the sub-interval travel cost is lower, ultimately resulting in the overall odor weight of the ICV navigation routes being higher than that of the DIJA and the FWA.

(1) For the ICV navigation routes "$P_{10,1,8,9}$", "$P_{10,8,1,9}$", and "$P_{8,1,10,9}$", the PRA has an overall odor weight 0.1456, 0.1448, and 0.1535 higher than the GDA, respectively, while the PRA has an overall travel cost 2.3024, 2.3985, and 3.6133 lower than the GDA, respectively. The cost optimization rates are 7.49%, 7.62%, and 10.20% to the GDA; the overall odor weight of the PRA is 0.2406, 0.2031, and 0.2367 higher than the BDA, while the PRA has an overall travel cost 5.1016, 3.2971, and 5.2914 lower than the BDA, respectively. The cost optimization rates are 15.22%, 10.19%, and 14.32% to the BDA.

(2) For the ICV navigation routes "$P_{10,1,8,9}$", "$P_{10,8,1,9}$", and "$P_{8,1,10,9}$", the PRA has an overall odor weight 0.2151, 0.1945, and 0.2110 higher than the DIJA, respectively, while the PRA has an overall travel cost 2.2028, 1.4005, and 2.3078 lower than the DIJA, respectively. The cost optimization rates are 7.19%, 4.59%, and 6.76% to the DIJA. The overall odor weight of the PRA is 0.0035, 0.0050, and 0.0078 higher than the FWA, while the PRA has an overall travel cost 0.2993, 0.3989, and 1.1075 lower than the FWA, respectively. The cost optimization rates are 1.05%, 1.36%, and 3.35% to the FWA.

Analyzing Figure 15, the comparison between the experimental group algorithm and the control group algorithm in the sub-interval odor weight and the overall odor weight difference of the ICV navigation route, the following conclusions are obtained:

(1) Comparing the PRA with the GDA, the maximum sub-interval difference occurs in the third sub-interval of the routes $P_{10,1,8,9}$ and $P_{10,8,1,9}$, as well as the second sub-interval of the route $P_{8,1,10,9}$, both of which are 0.0847. The maximum reduction in the

ICV travel cost occurs in the route $P_{8,1,10,9}$, with the PRA saving 10.20% travel cost compared to the GDA.

(2) Comparing the PRA with the BDA, the maximum sub-interval difference occurs in the third sub-interval of the routes $P_{10,1,8,9}$ and $P_{10,8,1,9}$, as well as the second sub-interval of the route $P_{8,1,10,9}$, both of which are 0.1140. The maximum reduction in the ICV travel cost occurs in the route $P_{10,1,8,9}$, with the PRA saving 15.22% travel cost compared to the BDA.

(3) Comparing the PRA with the DIJA, the maximum sub-interval difference occurs in the third sub-interval of the routes $P_{10,1,8,9}$ and $P_{10,1,8,9}$, as well as the second sub-interval of the route $P_{8,1,10,9}$, both of which are 0.0847. The maximum reduction in the ICV travel cost occurs in the route $P_{10,1,8,9}$, with the PRA saving 7.19% travel cost compared to the DIJA.

(4) Comparing the PRA with the FWA, the maximum sub-interval difference occurs in the fourth sub-interval of the route $P_{8,1,10,9}$, with a value of 0.0079. The maximum reduction in the ICV travel cost occurs in the route $P_{8,1,10,9}$, with the PRA saving 3.35% travel cost compared to the FWA.

Analyzing Figure 16, the comparison between the experimental group algorithm and the control group algorithms in terms of the sub-interval mileage difference and the total mileage difference of the ICV guidance route, the following conclusions are obtained:

(1) Comparing the PRA with the GDA, the maximum sub-interval difference occurs in the fourth sub-interval of the route $P_{8,1,10,9}$, with a value of 1.1075. The maximum reduction in the ICV travel cost occurs in the route $P_{8,1,10,9}$, with the PRA saving 10.20% travel cost compared to the GDA.

(2) Comparing the PRA with the BDA, the maximum sub-interval difference occurs in the first sub-interval of the route $P_{8,1,10,9}$, with a value of 1.7949. The maximum reduction in the ICV travel cost occurs in the route $P_{10,1,8,9}$, with the PRA saving 15.22% travel cost compared to the BDA.

(3) Comparing the PRA with the DIJA, the maximum sub-interval difference occurs in the fourth sub-interval of the route $P_{8,1,10,9}$, with a value of 1.1075. The maximum reduction in the ICV travel cost occurs in the route $P_{10,1,8,9}$, with the PRA saving 7.19% travel cost compared to the DIJA.

(4) Comparing the PRA with the FWA, the maximum sub-interval difference occurs in the fourth sub-interval of the route $P_{8,1,10,9}$, with a value of 1.1075. The maximum reduction in the ICV travel cost occurs in the route $P_{8,1,10,9}$, with the PRA saving 3.35% travel cost compared to the FWA.

Analyzing Table 12 and Figure 17, it can be concluded that the proposed algorithm has lower time complexity compared to the Dijkstra and the Floyd–Warshall. From the analysis of the changing trend, the Floyd–Warshall algorithm has the highest change level and speed in time complexity, which is the cubic level of nodes, followed by the Dijkstra algorithm, which is the square level of nodes. From the perspective of algorithm principle, the proposed algorithm traverses the entire feasible paths by searching all nodes within the sub-interval. During the flying process of the fruit fly group towards the current optimal individual, the number of searching times does not exceed the factorial $n!$ of the number of nodes n. After traversing all the feasible paths, the algorithm outputs the global optimal solution, so the time complexity does not exceed $O(n)$. The Dijkstra and Floyd–Warshall algorithms search for the shortest path in a different way. They explore the local optimal solutions by point-by-point searching, and consume more time. Therefore, the proposed algorithm has a superior advantage in searching for the global optimal solution compared to the control group algorithms.

Through comparative experiments, it can be concluded that the proposed algorithm is easier and definitely able to find the global optimal solution for the ICV navigation routes compared to the commonly used map route-planning methods and the traditional route-searching algorithms, which makes the ICV travel route in each sub-interval the shortest and has the highest odor concentration value, resulting in the highest odor concentration

value of the final output ICV navigation route. From the perspective of the total cost of the ICV navigation route, the proposed algorithm is superior to the traditional methods.

5. Conclusions and Future Work

5.1. Conclusions on the Research Work

The combination of the smart tourism and the intelligent connected vehicles to improve the tourism experience and the tourist satisfaction is one of the hot research topics in the field of intelligent connected vehicles. To improve tourist satisfaction, an ICV system must recommend the POIs that best meet tourists' interests and needs, and guide the ICV to the destination along the tour route with the lowest travel cost. Therefore, the symmetrical relationship between the POI attributes and the tourist interests is the key to recommending POIs; that is, the ICV decision-making system must use the tourist interests as the standard to match the POIs that meet both the feature attributes and the spatial attributes, so as to create a symmetrical relationship between the tourist interests and the POI attributes. Based on this idea, we construct a navigation route-planning model for the tourism intelligent connected vehicle based on the symmetrical spatial clustering and the improved fruit fly optimization algorithm.

Firstly, a POI feature attribute clustering algorithm based on the spatial decision forest is constructed, which utilizes the principle of symmetry to match the tourist's interests with the POI feature attributes. It is then used as an embedded algorithm in the ICV decision-making system to achieve the optimal POI feature attribute recommendation. Secondly, we construct a POI spatial attribute clustering algorithm based on the SA-AGNES, with the ICV transfer stations as seed points and the spatial accessibility as the objective function, to achieve the spatial modeling of the POI and ICV cluster. By determining the POI feature attributes weight and the spatial attribute weight based on the tourists, a POI recommendation algorithm for the ICV navigation route is constructed based on the attribute weights, and the POIs on the ICV navigation route are output. On this basis, we construct a tourism ICV navigation route model based on an improved fruit fly optimization algorithm, with the ICV transfer stations and the POIs as nodes, and output the navigation route with the lowest travel cost under the geospatial constraints. Finally, we design the validation experiment and comparative experiment, which prove that the proposed algorithm can accurately output the POIs that match the tourists' interests, and can find out the ICV navigation route with the lowest travel cost. Compared with the commonly used map route-planning methods and the traditional route-searching algorithms, our algorithm has better performance in searching for the global optimal solutions, and can find out the shortest path in each sub-interval of the ICV navigation route, then minimize the total travel cost of the ICV navigation route. Compared to the three optimal ICV navigation routes output by the traditional methods, the proposed algorithm can reduce the travel costs by 15.22% at most, which can also effectively reduce the energy consumption of the ICV system, and improve the efficiency of sight-seeing and traveling for tourists.

5.2. Limitations and Future Work

The proposed algorithm has certain prerequisites; for instance, the input basic interest indicators, tourist locations, ICV transfer station locations, POI feature attributes, POI spatial attributes, and urban geospatial data, etc. Since the intelligent ICV system and the tourism recommendation system are two complex systems, the complexity of their combination is much higher. Therefore, our research is on a tourism ICV guidance route decision-making system under certain constraints, and it is difficult to consider and cover all the conditions of the ICV system, recommendation system, and tourism activities. Thus, it has certain application limitations. Firstly, the location selection of the ICV transfer station plays a decisive role in the POI clustering results and the spatial decision-making of the POI routes. Our work does not involve research on the impact of the ICV location selection on the POI route recommendation results. Secondly, the tourist interests are still the focus and core of tourism research. Different preferences of the tourists for the POI feature attributes

and spatial attributes may lead to different POI and route recommendation results. There is still a need for in-depth research on the weight of the tourist interests.

In response to the limitations of our research work, we will further explore the integration of the intelligent connected vehicles (ICV) and the smart tourism services from the following two aspects in future research. Firstly, we will further study the site selection problem of the ICV transfer stations. Combining the urban geospatial constraints and the POI spatial distributions, we will construct the model using the optimal geospatial locations of the ICV transfer stations to optimize the spatial range and the functional area of the cluster where the ICV transfer stations are located. Secondly, we will further study the relationships between the selection of the POI feature attribute weights and the spatial attribute weights by the tourists, and the final output ICV guidance routes. By constructing a control variable model, the impact of the different tourist needs and weight selections on the final recommended POIs and ICV guidance route results will be studied. It is necessary to find out the internal mechanism of the weight function model acting on the ICV guidance routes for better serving the optimization of the ICV decision-making systems.

5.3. Application Directions

Based on this future work, the proposed algorithm model has the following application prospects. Firstly, developing the decision-making system specifically for the ICV intelligent navigation and POI recommendation. After renting an ICV from the ICV transfer station, tourist passengers can obtain the POI recommendations and the optimal route navigation by inputting their travel needs. This guides tourists to visit the POIs while saving the travel costs. Secondly, it is beneficial to further expand the application scope of the ICV intelligent navigation system, expanding the target POI to other user-interested goals, such as applying to the ICV navigation systems for hotel recommendations and navigation, hospital recommendations and navigation, and cinema recommendations and navigation, etc. Thirdly, designing and developing electronic maps with comprehensive functions such as the ICV system operation, target recommendation, route navigation, and POI navigation, etc., which can be applied to the urban geographic information systems and urban map systems, providing services for urban tourism, cargo transportation, and public transportation, etc.

Author Contributions: Conceptualization, X.Z., J.P., B.W. and M.S.; methodology, X.Z. and J.P.; formal analysis, X.Z., B.W. and M.S.; writing—original draft preparation, X.Z. and B.W.; writing—review and editing, X.Z., J.P., B.W. and M.S.; funding acquisition, X.Z., J.P. and B.W. All authors have read and agreed to the published version of the manuscript.

Funding: This research was funded by the Key R&D Program of Sichuan Province, China (No. 2022YFG0034, 2023YFG0115), the "Construction of Zhang Daqian's Cultural and Tourism Resource Spatial Model Based on Feature Clustering" of the Humanities and Social Sciences (Zhang Daqian Research) Youth Project of the Sichuan Provincial Department of Education (No. ZDQ2023-15), the Cooperative Program of Sichuan University and Yibin (No. 2020CDYB-30), the Cooperative Program of Sichuan University and Zigong (2022CDZG-6), the Key Research Base of Region and Country of Sichuan Province, Center for Southeast Asian Economic and Culture Studies (No. DNY2301), the Leshan Science and Technology Plan Project (No. 22ZRKX025) and the National Natural Science Foundation of China (Grant No. 42101455).

Data Availability Statement: Data are contained within the article.

Conflicts of Interest: The authors declare no conflicts of interest.

References

1. Skarakis, N.; Georgia Skiniti, G.; Tournaki, S.; Tsoutsos, T. Necessity to Assess the Sustainability of Sensitive Ecosystems: A Comprehensive Review of Tourism Pressures and the Travel Cost Method. *Sustainability* **2023**, *15*, 12064. [CrossRef]
2. Telonis, G.; Panteli, A.; Boutsinas, B. A Point-of-Interest Recommender System for Tourist Groups Based on Cooperative Location Set Cover Problem. *Mathematics* **2023**, *11*, 3646. [CrossRef]

3. Mamad, L.; Mbow, M.; Khriss, I.; Jakimi, A. A Software Factory for Accelerating the Development of Recommender Systems in Smart Tourism Mobile Applications: An Overview. *Comput. Sci. Math. Forum.* **2023**, *6*, 4.
4. Ruan, L.; Kou, X.; Ge, J.; Long, Y.; Zhang, L. A Method of Directional Signs Location Selection and Content Generation in Scenic Areas. *ISPRS Int. J. Geo-Inf.* **2020**, *9*, 574. [CrossRef]
5. Hou, B.; Zhang, K.; Gong, Z.; Li, Q.; Zhou, J.; Zhang, J.; Fortelle, A. SoC-VRP: A Deep-Reinforcement-Learning-Based Vehicle Route Planning Mechanism for Service-Oriented Cooperative ITS. *Electronics* **2023**, *12*, 4191. [CrossRef]
6. Noussaiba, M.; Razaque, A.; Rahal, R. Heterogeneous Algorithm for Efficient-Path Detection and Congestion Avoidance for a Vehicular-Management System. *Sensors* **2023**, *23*, 5471. [CrossRef]
7. Wang, C.; Chen, S.; Zhao, Q.; Suo, Y. An Efficient End-to-End Obstacle Avoidance Path Planning Algorithm for Intelligent Vehicles Based on Improved Whale Optimization Algorithm. *Mathematics* **2023**, *11*, 1800. [CrossRef]
8. Liu, B.; Long, J.; Deng, M.; Yang, X.; Shi, Y. An Adaptive Route Planning Method of Connected Vehicles for Improving the Transport Efficiency. *ISPRS Int. J. Geo-Inf.* **2022**, *11*, 39. [CrossRef]
9. Kurdi, H.; Almuhalhel, S.; Elgibreen, H.; Qahmash, H.; Albatati, B.; Al-Salem, L.; Almoaiqel, G. Tide-Inspired Path Planning Algorithm for Autonomous Vehicles. *Remote Sens.* **2021**, *13*, 4644. [CrossRef]
10. Xu, X.; Wang, L.; Zhang, S.; Li, W.; Jiang, Q. Modelling and Optimization of Personalized Scenic Tourism Routes Based on Urgency. *Appl. Sci.* **2023**, *13*, 2030. [CrossRef]
11. Shan, H. A Novel Travel Route Planning Method based on an Ant Colony Optimization Algorithm. *Open Geosci.* **2023**, *15*, 20220541.
12. Damos, M.A.; Zhu, J.; Li, W.; Hassan, A.; Khalifa, E. A Novel Urban Tourism Path Planning Approach Based on a Multiobjective Genetic Algorithm. *ISPRS Int. J. Geo-Inf.* **2021**, *10*, 530. [CrossRef]
13. Alshamlan, H.; Alghofaili, G.; ALFulayj, N.; Aldawsari, S.; Alrubaiya, Y.; Alabduljabbar, R. Promoting Sustainable Travel Experiences: A Weighted Parallel Hybrid Approach for Personalized Tourism Recommendations and Enhanced User Satisfaction. *Sustainability* **2023**, *15*, 14447. [CrossRef]
14. Zhou, K.; Yao, Z. Analysis of Customer Satisfaction in Tourism Services Based on the Kano Model. *Systems* **2023**, *11*, 345. [CrossRef]
15. Jiang, G.; Gao, W.; Xu, M.; Tong, M.; Liu, Z. Geographic Information Visualization and Sustainable Development of Low-Carbon Rural Slow Tourism under Artificial Intelligence. *Sustainability* **2023**, *15*, 3846. [CrossRef]
16. Riswanto, A.; Kim, S.; Kim, H. Analyzing Online Reviews to Uncover Customer Satisfaction Factors in Indian Cultural Tourism Destinations. *Behav. Sci.* **2023**, *13*, 923. [CrossRef]
17. Zhao, T.; Wang, Z.; Yong, Z.; Xu, P.; Wang, Q.; Du, X. The Spatiotemporal Pattern Evolution and Driving Force of Tourism Information Flow in the Chengdu–Chongqing City Cluster. *ISPRS Int. J. Geo-Inf.* **2023**, *12*, 414. [CrossRef]
18. Zhang, B.; Zhou, L.; Yin, Z.; Zhou, A.; Li, J. Study on the Correlation Characteristics between Scenic Byway Network Accessibility and Self-Driving Tourism Spatial Behavior in Western Sichuan. *Sustainability* **2023**, *15*, 14167. [CrossRef]
19. Sarna, N.; Ahmed, M.; Rithen, F.; Islam, M. A Framework of Vehicle Usage Optimization for Tour Purposes. *Appl. Sci.* **2023**, *13*, 10973. [CrossRef]
20. Ko, Y.; Ko, Y. A Development of Optimal Design and Operation Algorithm for Battery-Powered Electric City Tour Bus System. *Energies* **2023**, *16*, 1100. [CrossRef]
21. Li, J.; Tian, S.; Zhang, N.; Liu, G.; Wu, Z.; Li, W. Optimization Strategy for Electric Vehicle Routing under Traffic Impedance Guidance. *Appl. Sci.* **2023**, *13*, 11474. [CrossRef]
22. Zhong, Y.; Ye, S.; Liu, Y.; Li, J. A Route Planning Method for UAV Swarm Inspection of Roads Fusing Distributed Droneport Site Selection. *Sensors* **2023**, *23*, 8479. [CrossRef] [PubMed]